Understanding Binary Black Holes Through Gravitational Wave Detections

M. Benacquista
University of Texas Rio Grande Valley
Center for Gravitational Wave Astronomy

UTRGV

Wilhelm und Else Heraeus Stiftung

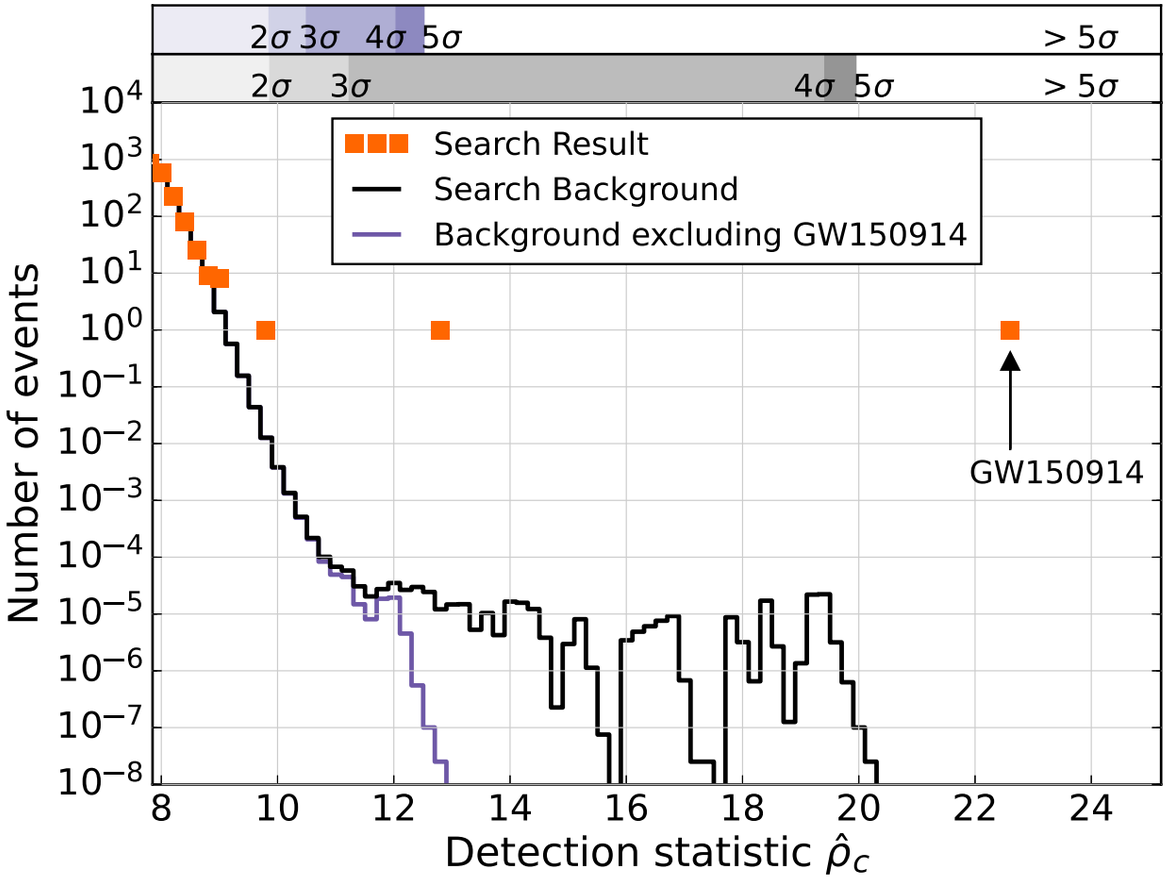
2σ 3σ 4σ 5σ
> 5σ
2σ 3σ 4σ 5σ
> 5σ
Search Result
Search Background
Background excluding GW150914
GW150914
Number of events
Detection statistic $\hat{\rho}_c$

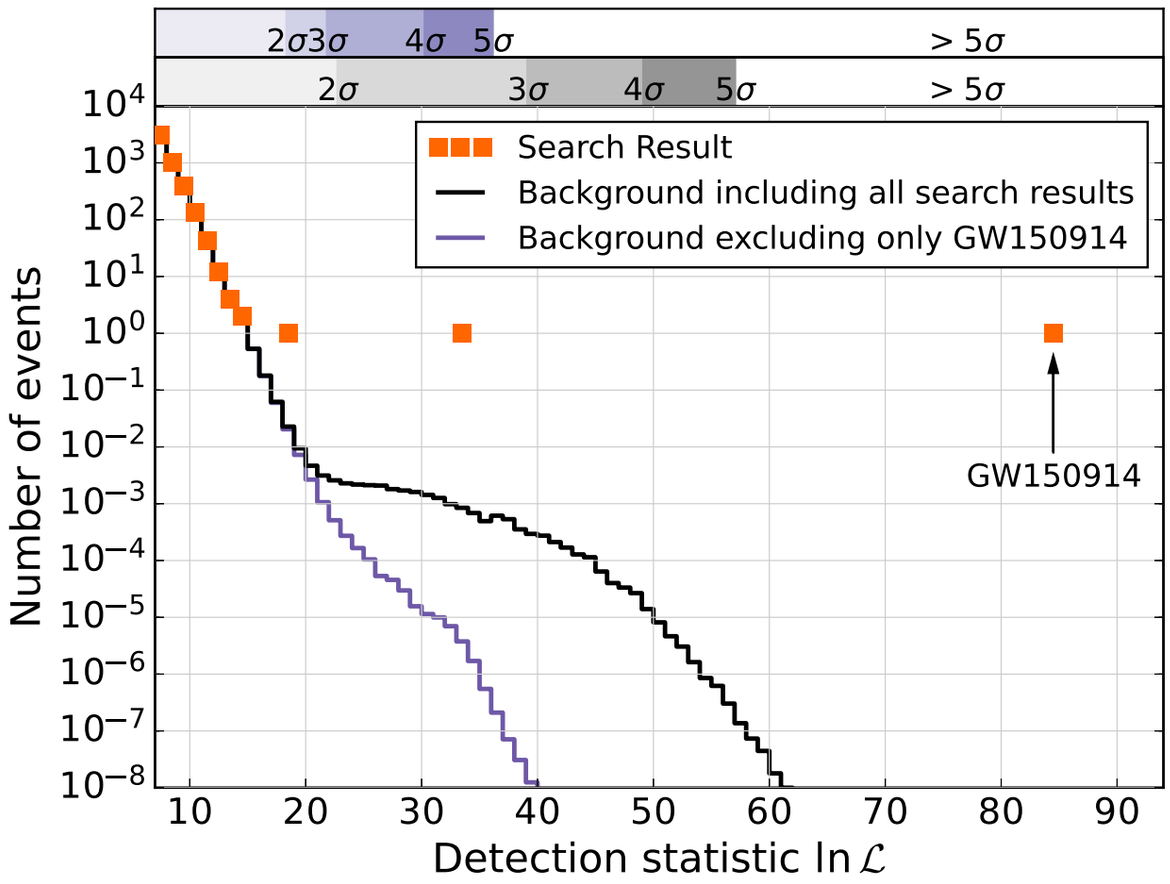
2σ 3σ 4σ 5σ
> 5σ
2σ 3σ 4σ 5σ
> 5σ
Search Result
Background including all search results
Background excluding only GW150914
GW150914
Number of events
Detection statistic ln $\mathcal{L}$

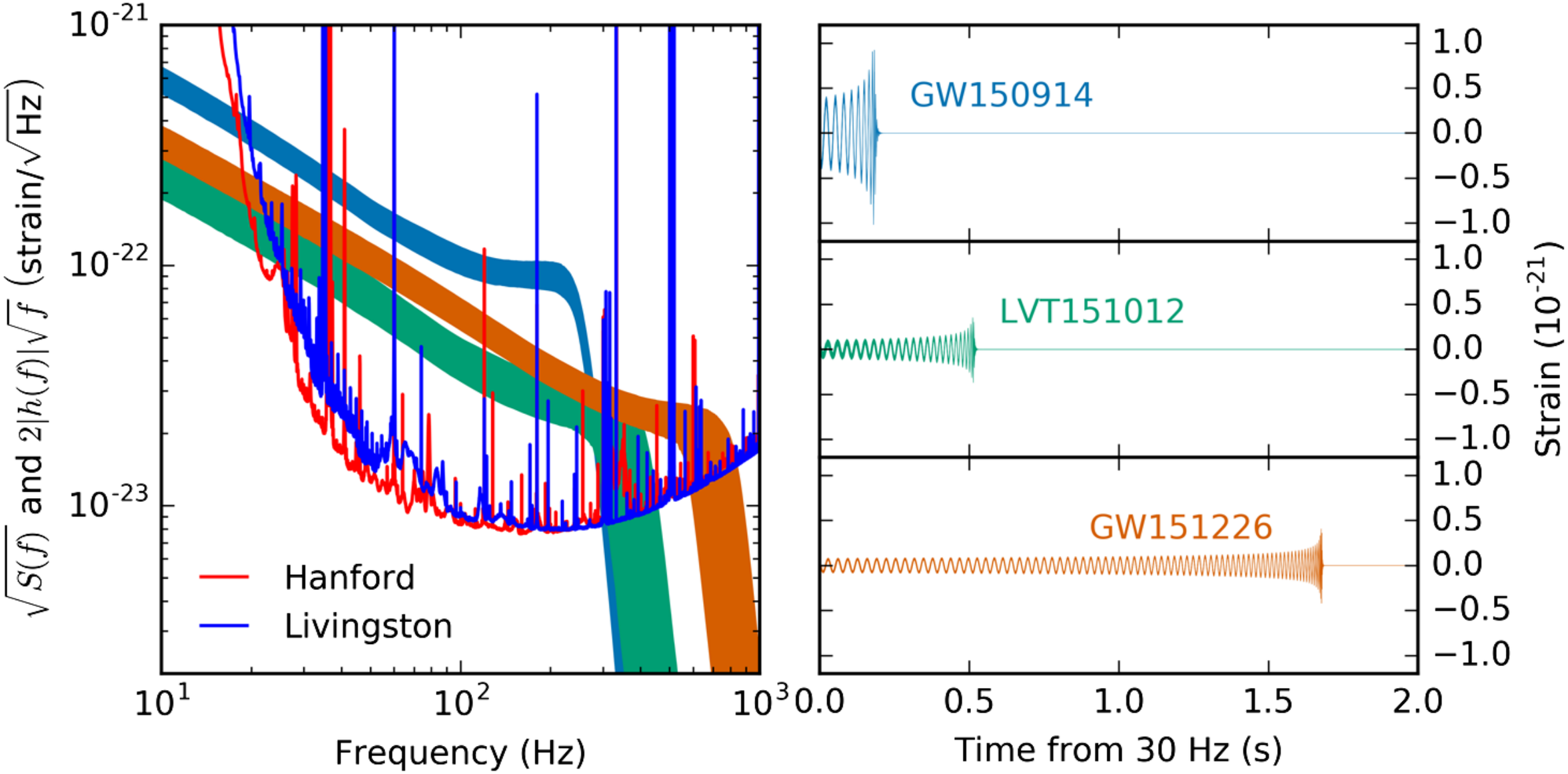
10^{-21}
10^{-22}
10^{-23}
$\sqrt{S(f)}$ and $2|h(f)|\sqrt{f}$ (strain/$\sqrt{\text{Hz}}$)
Hanford
Livingston
10^1
10^2
10^3
Frequency (Hz)
GW150914
LVT151012
GW151226
1.0
0.5
0.0
−0.5
−1.0
Strain (10^{-21})
0.0
0.5
1.0
1.5
2.0
Time from 30 Hz (s)

	GW150914			GW151226			LVT151012		
	EOBNR	IMRPhenom	Overall	EOBNR	IMRPhenom	Overall	EOBNR	IMRPhenom	Overall
Detector frame									
Total mass $M/\mathrm{M}_\odot$	$71.0^{+4.6}_{-4.0}$	$71.2^{+3.5}_{-3.2}$	$71.1^{+4.1\pm0.7}_{-3.6\pm0.8}$	$23.6^{+8.0}_{-1.3}$	$23.8^{+5.1}_{-1.5}$	$23.7^{+6.5\pm2.2}_{-1.4\pm0.1}$	45^{+17}_{-4}	44^{+12}_{-3}	$44^{+16\pm5}_{-3\pm0}$
Chirp mass $\mathcal{M}/\mathrm{M}_\odot$	$30.4^{+2.3}_{-1.6}$	$30.7^{+1.5}_{-1.5}$	$30.6^{+1.9\pm0.3}_{-1.6\pm0.4}$	$9.71^{+0.08}_{-0.07}$	$9.72^{+0.06}_{-0.06}$	$9.72^{+0.07\pm0.01}_{-0.06\pm0.01}$	$18.1^{+1.3}_{-0.9}$	$18.1^{+0.8}_{-0.8}$	$18.1^{+1.0\pm0.5}_{-0.8\pm0.1}$
Primary mass $m_1/\mathrm{M}_\odot$	$40.2^{+5.2}_{-4.8}$	$38.5^{+5.4}_{-3.3}$	$39.4^{+5.4\pm1.3}_{-4.1\pm0.2}$	$15.3^{+10.8}_{-3.8}$	$15.8^{+7.2}_{-4.0}$	$15.6^{+9.0\pm2.6}_{-4.0\pm0.2}$	29^{+23}_{-8}	27^{+19}_{-6}	$28^{+21\pm5}_{-7\pm0}$
Secondary mass $m_2/\mathrm{M}_\odot$	$30.6^{+5.1}_{-4.2}$	$32.7^{+3.1}_{-4.9}$	$31.7^{+4.0\pm0.1}_{-4.9\pm1.2}$	$8.3^{+2.5}_{-2.9}$	$8.1^{+2.5}_{-2.1}$	$8.2^{+2.6\pm0.2}_{-2.5\pm0.5}$	15^{+5}_{-6}	16^{+4}_{-6}	$16^{+5\pm0}_{-6\pm1}$
Final mass $M_\mathrm{f}/\mathrm{M}_\odot$	$67.8^{+4.0}_{-3.6}$	$67.9^{+3.2}_{-2.9}$	$67.8^{+3.7\pm0.6}_{-3.3\pm0.7}$	$22.5^{+8.2}_{-1.4}$	$22.8^{+5.3}_{-1.6}$	$22.6^{+6.7\pm2.2}_{-1.5\pm0.1}$	43^{+17}_{-4}	42^{+13}_{-2}	$42^{+16\pm5}_{-3\pm0}$
Source frame									
Total mass $M^\mathrm{source}/\mathrm{M}_\odot$	$65.5^{+4.4}_{-3.9}$	$65.1^{+3.6}_{-3.1}$	$65.3^{+4.1\pm1.0}_{-3.4\pm0.3}$	$21.6^{+7.4}_{-1.6}$	$21.9^{+4.7}_{-1.7}$	$21.8^{+5.9\pm2.0}_{-1.7\pm0.1}$	38^{+15}_{-5}	37^{+11}_{-4}	$37^{+13\pm4}_{-4\pm0}$
Chirp mass $\mathcal{M}^\mathrm{source}/\mathrm{M}_\odot$	$28.1^{+2.1}_{-1.6}$	$28.1^{+1.6}_{-1.4}$	$28.1^{+1.8\pm0.4}_{-1.5\pm0.2}$	$8.87^{+0.35}_{-0.28}$	$8.90^{+0.31}_{-0.27}$	$8.88^{+0.33\pm0.01}_{-0.28\pm0.04}$	$15.2^{+1.5}_{-1.1}$	$15.0^{+1.3}_{-1.0}$	$15.1^{+1.4\pm0.3}_{-1.1\pm0.0}$
Primary mass $m_1^\mathrm{source}/\mathrm{M}_\odot$	$37.0^{+4.9}_{-4.4}$	$35.3^{+5.1}_{-3.1}$	$36.2^{+5.2\pm1.4}_{-3.8\pm0.4}$	$14.0^{+10.0}_{-3.5}$	$14.5^{+6.6}_{-3.7}$	$14.2^{+8.3\pm2.4}_{-3.7\pm0.2}$	24^{+19}_{-7}	23^{+16}_{-5}	$23^{+18\pm5}_{-6\pm0}$
Secondary mass $m_2^\mathrm{source}/\mathrm{M}_\odot$	$28.3^{+4.6}_{-3.9}$	$29.9^{+3.0}_{-4.5}$	$29.1^{+3.7\pm0.0}_{-4.4\pm0.9}$	$7.5^{+2.3}_{-2.6}$	$7.4^{+2.3}_{-2.0}$	$7.5^{+2.3\pm0.2}_{-2.3\pm0.4}$	13^{+4}_{-5}	14^{+4}_{-5}	$13^{+4\pm0}_{-5\pm0}$
Final mass $M_\mathrm{f}^\mathrm{source}/\mathrm{M}_\odot$	$62.5^{+3.9}_{-3.5}$	$62.1^{+3.3}_{-2.8}$	$62.3^{+3.7\pm0.9}_{-3.1\pm0.2}$	$20.6^{+7.6}_{-1.6}$	$20.9^{+4.8}_{-1.8}$	$20.8^{+6.1\pm2.0}_{-1.7\pm0.1}$	36^{+15}_{-4}	35^{+11}_{-3}	$35^{+14\pm4}_{-4\pm0}$
Energy radiated $E_\mathrm{rad}/(\mathrm{M}_\odot c^2)$	$2.98^{+0.55}_{-0.40}$	$3.02^{+0.36}_{-0.36}$	$3.00^{+0.47\pm0.13}_{-0.39\pm0.07}$	$1.02^{+0.09}_{-0.24}$	$0.99^{+0.11}_{-0.17}$	$1.00^{+0.10\pm0.01}_{-0.20\pm0.03}$	$1.48^{+0.39}_{-0.41}$	$1.51^{+0.29}_{-0.44}$	$1.50^{+0.33\pm0.05}_{-0.43\pm0.01}$
Mass ratio q	$0.77^{+0.20}_{-0.18}$	$0.85^{+0.13}_{-0.21}$	$0.81^{+0.17\pm0.02}_{-0.20\pm0.04}$	$0.54^{+0.40}_{-0.33}$	$0.51^{+0.39}_{-0.25}$	$0.52^{+0.40\pm0.03}_{-0.29\pm0.04}$	$0.53^{+0.42}_{-0.34}$	$0.60^{+0.35}_{-0.37}$	$0.57^{+0.38\pm0.01}_{-0.37\pm0.04}$
Effective inspiral spin χ_eff	$-0.08^{+0.17}_{-0.14}$	$-0.05^{+0.11}_{-0.12}$	$-0.06^{+0.14\pm0.02}_{-0.14\pm0.04}$	$0.21^{+0.24}_{-0.11}$	$0.22^{+0.15}_{-0.08}$	$0.21^{+0.20\pm0.07}_{-0.10\pm0.03}$	$0.06^{+0.31}_{-0.24}$	$0.01^{+0.26}_{-0.17}$	$0.03^{+0.31\pm0.08}_{-0.20\pm0.02}$
Primary spin magnitude a_1	$0.33^{+0.39}_{-0.29}$	$0.30^{+0.54}_{-0.27}$	$0.32^{+0.47\pm0.10}_{-0.29\pm0.01}$	$0.42^{+0.35}_{-0.37}$	$0.55^{+0.35}_{-0.42}$	$0.49^{+0.37\pm0.11}_{-0.42\pm0.07}$	$0.31^{+0.46}_{-0.27}$	$0.31^{+0.50}_{-0.28}$	$0.31^{+0.48\pm0.03}_{-0.28\pm0.00}$
Secondary spin magnitude a_2	$0.62^{+0.35}_{-0.54}$	$0.36^{+0.53}_{-0.33}$	$0.48^{+0.47\pm0.08}_{-0.43\pm0.03}$	$0.51^{+0.44}_{-0.46}$	$0.52^{+0.42}_{-0.47}$	$0.52^{+0.43\pm0.01}_{-0.47\pm0.00}$	$0.49^{+0.45}_{-0.44}$	$0.42^{+0.50}_{-0.38}$	$0.45^{+0.48\pm0.02}_{-0.41\pm0.01}$
Final spin a_f	$0.68^{+0.05}_{-0.07}$	$0.68^{+0.06}_{-0.05}$	$0.68^{+0.05\pm0.01}_{-0.06\pm0.02}$	$0.73^{+0.05}_{-0.06}$	$0.75^{+0.07}_{-0.05}$	$0.74^{+0.06\pm0.03}_{-0.06\pm0.03}$	$0.65^{+0.09}_{-0.10}$	$0.66^{+0.08}_{-0.10}$	$0.66^{+0.09\pm0.00}_{-0.10\pm0.02}$
Luminosity distance $D_\mathrm{L}/\mathrm{Mpc}$	400^{+160}_{-180}	440^{+140}_{-170}	$420^{+150\pm20}_{-180\pm40}$	450^{+180}_{-210}	440^{+170}_{-180}	$440^{+180\pm20}_{-190\pm10}$	1000^{+540}_{-490}	1030^{+480}_{-480}	$1020^{+500\pm20}_{-490\pm40}$
Source redshift z	$0.086^{+0.031}_{-0.036}$	$0.094^{+0.027}_{-0.034}$	$0.090^{+0.029\pm0.003}_{-0.036\pm0.008}$	$0.096^{+0.035}_{-0.042}$	$0.092^{+0.033}_{-0.037}$	$0.094^{+0.035\pm0.004}_{-0.039\pm0.001}$	$0.198^{+0.091}_{-0.092}$	$0.204^{+0.082}_{-0.088}$	$0.201^{+0.086\pm0.003}_{-0.091\pm0.008}$
Upper bound									
Primary spin magnitude a_1	0.62	0.73	0.67 ± 0.09	0.68	0.83	0.77 ± 0.12	0.64	0.69	0.67 ± 0.04
Secondary spin magnitude a_2	0.93	0.80	0.90 ± 0.12	0.90	0.89	0.90 ± 0.01	0.89	0.85	0.87 ± 0.04
Lower bound									
Mass ratio q	0.62	0.68	0.65 ± 0.05	0.25	0.30	0.28 ± 0.04	0.22	0.28	0.24 ± 0.05
Log Bayes factor $\ln \mathcal{B}_{\mathrm{s/n}}$	287.7 ± 0.1	289.8 ± 0.3	⋯	59.5 ± 0.1	60.2 ± 0.2	⋯	22.8 ± 0.2	23.0 ± 0.1	⋯
Information criterion DIC	32977.2 ± 0.3	32973.1 ± 0.1	⋯	34296.4 ± 0.2	34295.1 ± 0.1	⋯	94695.8 ± 0.0	94692.9 ± 0.0	⋯

M M_1 M_2

	GW150914			GW151226			LVT151012		
	EOBNR	IMRPhenom	Overall	EOBNR	IMRPhenom	Overall	EOBNR	IMRPhenom	Overall
Detector frame									
Total mass $M/\mathrm{M}_\odot$	$71.0^{+4.6}_{-4.0}$	$71.2^{+3.5}_{-3.2}$	$71.1^{+4.1\pm0.7}_{-3.6\pm0.8}$	$23.6^{+8.0}_{-1.3}$	$23.8^{+5.1}_{-1.5}$	$23.7^{+6.5\pm2.2}_{-1.4\pm0.1}$	45^{+17}_{-4}	44^{+12}_{-3}	$44^{+16\pm5}_{-3\pm0}$
Chirp mass $\mathcal{M}/\mathrm{M}_\odot$	$30.4^{+2.3}_{-1.6}$	$30.7^{+1.5}_{-1.5}$	$30.6^{+1.9\pm0.3}_{-1.6\pm0.4}$	$9.71^{+0.08}_{-0.07}$	$9.72^{+0.06}_{-0.06}$	$9.72^{+0.07\pm0.01}_{-0.06\pm0.01}$	$18.1^{+1.3}_{-0.9}$	$18.1^{+0.8}_{-0.8}$	$18.1^{+1.0\pm0.5}_{-0.8\pm0.1}$
Primary mass $m_1/\mathrm{M}_\odot$	$40.2^{+5.2}_{-4.8}$	$38.5^{+5.4}_{-3.3}$	$39.4^{+5.4\pm1.3}_{-4.1\pm0.2}$	$15.3^{+10.8}_{-3.8}$	$15.8^{+7.2}_{-4.0}$	$15.6^{+9.0\pm2.6}_{-4.0\pm0.2}$	29^{+23}_{-8}	27^{+19}_{-6}	$28^{+21\pm5}_{-7\pm0}$
Secondary mass $m_2/\mathrm{M}_\odot$	$30.6^{+5.1}_{-4.2}$	$32.7^{+3.1}_{-4.9}$	$31.7^{+4.0\pm0.1}_{-4.9\pm1.2}$	$8.3^{+2.5}_{-2.9}$	$8.1^{+2.5}_{-2.1}$	$8.2^{+2.6\pm0.2}_{-2.5\pm0.5}$	15^{+5}_{-6}	16^{+4}_{-6}	$16^{+5\pm0}_{-6\pm1}$
Final mass $M_\mathrm{f}/\mathrm{M}_\odot$	$67.8^{+4.0}_{-3.6}$	$67.9^{+3.2}_{-2.9}$	$67.8^{+3.7\pm0.6}_{-3.3\pm0.7}$	$22.5^{+8.2}_{-1.4}$	$22.8^{+5.3}_{-1.6}$	$22.6^{+6.7\pm2.2}_{-1.5\pm0.1}$	43^{+17}_{-4}	42^{+13}_{-2}	$42^{+16\pm5}_{-3\pm0}$
Source frame									
Total mass $M^\mathrm{source}/\mathrm{M}_\odot$	$65.5^{+4.4}_{-3.9}$	$65.1^{+3.6}_{-3.1}$	$65.3^{+4.1\pm1.0}_{-3.4\pm0.3}$	$21.6^{+7.4}_{-1.6}$	$21.9^{+4.7}_{-1.7}$	$21.8^{+5.9\pm2.0}_{-1.7\pm0.1}$	38^{+15}_{-5}	37^{+11}_{-4}	$37^{+13\pm4}_{-4\pm0}$
Chirp mass $\mathcal{M}^\mathrm{source}/\mathrm{M}_\odot$	$28.1^{+2.1}_{-1.6}$	$28.1^{+1.6}_{-1.4}$	$28.1^{+1.8\pm0.4}_{-1.5\pm0.2}$	$8.87^{+0.35}_{-0.28}$	$8.90^{+0.31}_{-0.27}$	$8.88^{+0.33\pm0.01}_{-0.28\pm0.04}$	$15.2^{+1.5}_{-1.1}$	$15.0^{+1.3}_{-1.0}$	$15.1^{+1.4\pm0.3}_{-1.1\pm0.0}$
Primary mass $m_1^\mathrm{source}/\mathrm{M}_\odot$	$37.0^{+4.9}_{-4.4}$	$35.3^{+5.1}_{-3.1}$	$36.2^{+5.2\pm1.4}_{-3.8\pm0.4}$	$14.0^{+10.0}_{-3.5}$	$14.5^{+6.6}_{-3.7}$	$14.2^{+8.3\pm2.4}_{-3.7\pm0.2}$	24^{+19}_{-7}	23^{+16}_{-5}	$23^{+18\pm5}_{-6\pm0}$
Secondary mass $m_2^\mathrm{source}/\mathrm{M}_\odot$	$28.3^{+4.6}_{-3.9}$	$29.9^{+3.0}_{-4.5}$	$29.1^{+3.7\pm0.0}_{-4.4\pm0.9}$	$7.5^{+2.3}_{-2.6}$	$7.4^{+2.3}_{-2.0}$	$7.5^{+2.3\pm0.2}_{-2.3\pm0.4}$	13^{+4}_{-5}	14^{+4}_{-5}	$13^{+4\pm0}_{-5\pm0}$
Final mass $M_\mathrm{f}^\mathrm{source}/\mathrm{M}_\odot$	$62.5^{+3.9}_{-3.5}$	$62.1^{+3.3}_{-2.8}$	$62.3^{+3.7\pm0.9}_{-3.1\pm0.2}$	$20.6^{+7.6}_{-1.6}$	$20.9^{+4.8}_{-1.8}$	$20.8^{+6.1\pm2.0}_{-1.7\pm0.1}$	36^{+15}_{-4}	35^{+11}_{-3}	$35^{+14\pm4}_{-4\pm0}$
Energy radiated $E_\mathrm{rad}/(\mathrm{M}_\odot c^2)$	$2.98^{+0.55}_{-0.40}$	$3.02^{+0.36}_{-0.36}$	$3.00^{+0.47\pm0.13}_{-0.39\pm0.07}$	$1.02^{+0.09}_{-0.24}$	$0.99^{+0.11}_{-0.17}$	$1.00^{+0.10\pm0.01}_{-0.20\pm0.03}$	$1.48^{+0.39}_{-0.41}$	$1.51^{+0.29}_{-0.44}$	$1.50^{+0.33\pm0.05}_{-0.43\pm0.01}$
Mass ratio q	$0.77^{+0.20}_{-0.18}$	$0.85^{+0.13}_{-0.21}$	$0.81^{+0.17\pm0.02}_{-0.20\pm0.04}$	$0.54^{+0.40}_{-0.33}$	$0.51^{+0.39}_{-0.25}$	$0.52^{+0.40\pm0.03}_{-0.29\pm0.04}$	$0.53^{+0.42}_{-0.34}$	$0.60^{+0.35}_{-0.37}$	$0.57^{+0.38\pm0.01}_{-0.37\pm0.04}$
Effective inspiral spin χ_eff	$-0.08^{+0.17}_{-0.14}$	$-0.05^{+0.11}_{-0.12}$	$-0.06^{+0.14\pm0.02}_{-0.14\pm0.04}$	$0.21^{+0.24}_{-0.11}$	$0.22^{+0.15}_{-0.08}$	$0.21^{+0.20\pm0.07}_{-0.10\pm0.03}$	$0.06^{+0.31}_{-0.24}$	$0.01^{+0.26}_{-0.17}$	$0.03^{+0.31\pm0.08}_{-0.20\pm0.02}$
Primary spin magnitude a_1	$0.33^{+0.39}_{-0.29}$	$0.30^{+0.54}_{-0.27}$	$0.32^{+0.47\pm0.10}_{-0.29\pm0.01}$	$0.42^{+0.35}_{-0.37}$	$0.55^{+0.35}_{-0.42}$	$0.49^{+0.37\pm0.11}_{-0.42\pm0.07}$	$0.31^{+0.46}_{-0.27}$	$0.31^{+0.50}_{-0.28}$	$0.31^{+0.48\pm0.03}_{-0.28\pm0.00}$
Secondary spin magnitude a_2	$0.62^{+0.35}_{-0.54}$	$0.36^{+0.53}_{-0.33}$	$0.48^{+0.47\pm0.08}_{-0.43\pm0.03}$	$0.51^{+0.44}_{-0.46}$	$0.52^{+0.42}_{-0.47}$	$0.52^{+0.43\pm0.01}_{-0.47\pm0.00}$	$0.49^{+0.45}_{-0.44}$	$0.42^{+0.50}_{-0.38}$	$0.45^{+0.48\pm0.02}_{-0.41\pm0.01}$
Final spin a_f	$0.68^{+0.05}_{-0.07}$	$0.68^{+0.06}_{-0.05}$	$0.68^{+0.05\pm0.01}_{-0.06\pm0.02}$	$0.73^{+0.05}_{-0.06}$	$0.75^{+0.07}_{-0.05}$	$0.74^{+0.06\pm0.03}_{-0.06\pm0.03}$	$0.65^{+0.09}_{-0.10}$	$0.66^{+0.08}_{-0.10}$	$0.66^{+0.09\pm0.00}_{-0.10\pm0.02}$
Luminosity distance $D_\mathrm{L}/\mathrm{Mpc}$	400^{+160}_{-180}	440^{+140}_{-170}	$420^{+150\pm20}_{-180\pm40}$	450^{+180}_{-210}	440^{+170}_{-180}	$440^{+180\pm20}_{-190\pm10}$	1000^{+540}_{-490}	1030^{+480}_{-480}	$1020^{+500\pm20}_{-490\pm40}$
Source redshift z	$0.086^{+0.031}_{-0.036}$	$0.094^{+0.027}_{-0.034}$	$0.090^{+0.029\pm0.003}_{-0.036\pm0.008}$	$0.096^{+0.035}_{-0.042}$	$0.092^{+0.033}_{-0.037}$	$0.094^{+0.035\pm0.004}_{-0.039\pm0.001}$	$0.198^{+0.091}_{-0.092}$	$0.204^{+0.082}_{-0.088}$	$0.201^{+0.086\pm0.003}_{-0.091\pm0.008}$
Upper bound									
Primary spin magnitude a_1	0.62	0.73	0.67 ± 0.09	0.68	0.83	0.77 ± 0.12	0.64	0.69	0.67 ± 0.04
Secondary spin magnitude a_2	0.93	0.80	0.90 ± 0.12	0.90	0.89	0.90 ± 0.01	0.89	0.85	0.87 ± 0.04
Lower bound									
Mass ratio q	0.62	0.68	0.65 ± 0.05	0.25	0.30	0.28 ± 0.04	0.22	0.28	0.24 ± 0.05
Log Bayes factor $\ln \mathcal{B}_{\mathrm{s/n}}$	287.7 ± 0.1	289.8 ± 0.3	⋯	59.5 ± 0.1	60.2 ± 0.2	⋯	22.8 ± 0.2	23.0 ± 0.1	⋯
Information criterion DIC	32977.2 ± 0.3	32973.1 ± 0.1	⋯	34296.4 ± 0.2	34295.1 ± 0.1	⋯	94695.8 ± 0.0	94692.9 ± 0.0	⋯

M M_1 M_2 65 36 29

	GW150914			GW151226			LVT151012		
	EOBNR	IMRPhenom	Overall	EOBNR	IMRPhenom	Overall	EOBNR	IMRPhenom	Overall
Detector frame									
Total mass $M/\mathrm{M}_\odot$	$71.0^{+4.6}_{-4.0}$	$71.2^{+3.5}_{-3.2}$	$71.1^{+4.1\pm0.7}_{-3.6\pm0.8}$	$23.6^{+8.0}_{-1.3}$	$23.8^{+5.1}_{-1.5}$	$23.7^{+6.5\pm2.2}_{-1.4\pm0.1}$	45^{+17}_{-4}	44^{+12}_{-3}	$44^{+16\pm5}_{-3\pm0}$
Chirp mass $\mathcal{M}/\mathrm{M}_\odot$	$30.4^{+2.3}_{-1.6}$	$30.7^{+1.5}_{-1.5}$	$30.6^{+1.9\pm0.3}_{-1.6\pm0.4}$	$9.71^{+0.08}_{-0.07}$	$9.72^{+0.06}_{-0.06}$	$9.72^{+0.07\pm0.01}_{-0.06\pm0.01}$	$18.1^{+1.3}_{-0.9}$	$18.1^{+0.8}_{-0.8}$	$18.1^{+1.0\pm0.5}_{-0.8\pm0.1}$
Primary mass $m_1/\mathrm{M}_\odot$	$40.2^{+5.2}_{-4.8}$	$38.5^{+5.4}_{-3.3}$	$39.4^{+5.4\pm1.3}_{-4.1\pm0.2}$	$15.3^{+10.8}_{-3.8}$	$15.8^{+7.2}_{-4.0}$	$15.6^{+9.0\pm2.6}_{-4.0\pm0.2}$	29^{+23}_{-8}	27^{+19}_{-6}	$28^{+21\pm5}_{-7\pm0}$
Secondary mass $m_2/\mathrm{M}_\odot$	$30.6^{+5.1}_{-4.2}$	$32.7^{+3.1}_{-4.9}$	$31.7^{+4.0\pm0.1}_{-4.9\pm1.2}$	$8.3^{+2.5}_{-2.9}$	$8.1^{+2.5}_{-2.1}$	$8.2^{+2.6\pm0.2}_{-2.5\pm0.5}$	15^{+5}_{-6}	16^{+4}_{-6}	$16^{+5\pm0}_{-6\pm1}$
Final mass $M_\mathrm{f}/\mathrm{M}_\odot$	$67.8^{+4.0}_{-3.6}$	$67.9^{+3.2}_{-2.9}$	$67.8^{+3.7\pm0.6}_{-3.3\pm0.7}$	$22.5^{+8.2}_{-1.4}$	$22.8^{+5.3}_{-1.6}$	$22.6^{+6.7\pm2.2}_{-1.5\pm0.1}$	43^{+17}_{-4}	42^{+13}_{-2}	$42^{+16\pm5}_{-3\pm0}$
Source frame									
Total mass $M^\mathrm{source}/\mathrm{M}_\odot$	$65.5^{+4.4}_{-3.9}$	$65.1^{+3.6}_{-3.1}$	$65.3^{+4.1\pm1.0}_{-3.4\pm0.3}$	$21.6^{+7.4}_{-1.6}$	$21.9^{+4.7}_{-1.7}$	$21.8^{+5.9\pm2.0}_{-1.7\pm0.1}$	38^{+15}_{-5}	37^{+11}_{-4}	$37^{+13\pm4}_{-4\pm0}$
Chirp mass $\mathcal{M}^\mathrm{source}/\mathrm{M}_\odot$	$28.1^{+2.1}_{-1.6}$	$28.1^{+1.6}_{-1.4}$	$28.1^{+1.8\pm0.4}_{-1.5\pm0.2}$	$8.87^{+0.35}_{-0.28}$	$8.90^{+0.31}_{-0.27}$	$8.88^{+0.33\pm0.01}_{-0.28\pm0.04}$	$15.2^{+1.5}_{-1.1}$	$15.0^{+1.3}_{-1.0}$	$15.1^{+1.4\pm0.3}_{-1.1\pm0.0}$
Primary mass $m_1^\mathrm{source}/\mathrm{M}_\odot$	$37.0^{+4.9}_{-4.4}$	$35.3^{+5.1}_{-3.1}$	$36.2^{+5.2\pm1.4}_{-3.8\pm0.4}$	$14.0^{+10.0}_{-3.5}$	$14.5^{+6.6}_{-3.7}$	$14.2^{+8.3\pm2.4}_{-3.7\pm0.2}$	24^{+19}_{-7}	23^{+16}_{-5}	$23^{+18\pm5}_{-6\pm0}$
Secondary mass $m_2^\mathrm{source}/\mathrm{M}_\odot$	$28.3^{+4.6}_{-3.9}$	$29.9^{+3.0}_{-4.5}$	$29.1^{+3.7\pm0.0}_{-4.4\pm0.9}$	$7.5^{+2.3}_{-2.6}$	$7.4^{+2.3}_{-2.0}$	$7.5^{+2.3\pm0.2}_{-2.3\pm0.4}$	13^{+4}_{-5}	14^{+4}_{-5}	$13^{+4\pm0}_{-5\pm0}$
Final mass $M_\mathrm{f}^\mathrm{source}/\mathrm{M}_\odot$	$62.5^{+3.9}_{-3.5}$	$62.1^{+3.3}_{-2.8}$	$62.3^{+3.7\pm0.9}_{-3.1\pm0.2}$	$20.6^{+7.6}_{-1.6}$	$20.9^{+4.8}_{-1.8}$	$20.8^{+6.1\pm2.0}_{-1.7\pm0.1}$	36^{+15}_{-4}	35^{+11}_{-3}	$35^{+14\pm4}_{-4\pm0}$
Energy radiated $E_\mathrm{rad}/(\mathrm{M}_\odot c^2)$	$2.98^{+0.55}_{-0.40}$	$3.02^{+0.36}_{-0.36}$	$3.00^{+0.47\pm0.13}_{-0.39\pm0.07}$	$1.02^{+0.09}_{-0.24}$	$0.99^{+0.11}_{-0.17}$	$1.00^{+0.10\pm0.01}_{-0.20\pm0.03}$	$1.48^{+0.39}_{-0.41}$	$1.51^{+0.29}_{-0.44}$	$1.50^{+0.33\pm0.05}_{-0.43\pm0.01}$
Mass ratio q	$0.77^{+0.20}_{-0.18}$	$0.85^{+0.13}_{-0.21}$	$0.81^{+0.17\pm0.02}_{-0.20\pm0.04}$	$0.54^{+0.40}_{-0.33}$	$0.51^{+0.39}_{-0.25}$	$0.52^{+0.40\pm0.03}_{-0.29\pm0.04}$	$0.53^{+0.42}_{-0.34}$	$0.60^{+0.35}_{-0.37}$	$0.57^{+0.38\pm0.01}_{-0.37\pm0.04}$
Effective inspiral spin χ_eff	$-0.08^{+0.17}_{-0.14}$	$-0.05^{+0.11}_{-0.12}$	$-0.06^{+0.14\pm0.02}_{-0.14\pm0.04}$	$0.21^{+0.24}_{-0.11}$	$0.22^{+0.15}_{-0.08}$	$0.21^{+0.20\pm0.07}_{-0.10\pm0.03}$	$0.06^{+0.31}_{-0.24}$	$0.01^{+0.26}_{-0.17}$	$0.03^{+0.31\pm0.08}_{-0.20\pm0.02}$
Primary spin magnitude a_1	$0.33^{+0.39}_{-0.29}$	$0.30^{+0.54}_{-0.27}$	$0.32^{+0.47\pm0.10}_{-0.29\pm0.01}$	$0.42^{+0.35}_{-0.37}$	$0.55^{+0.35}_{-0.42}$	$0.49^{+0.37\pm0.11}_{-0.42\pm0.07}$	$0.31^{+0.46}_{-0.27}$	$0.31^{+0.50}_{-0.28}$	$0.31^{+0.48\pm0.03}_{-0.28\pm0.00}$
Secondary spin magnitude a_2	$0.62^{+0.35}_{-0.54}$	$0.36^{+0.53}_{-0.33}$	$0.48^{+0.47\pm0.08}_{-0.43\pm0.03}$	$0.51^{+0.44}_{-0.46}$	$0.52^{+0.42}_{-0.47}$	$0.52^{+0.43\pm0.01}_{-0.47\pm0.00}$	$0.49^{+0.45}_{-0.44}$	$0.42^{+0.50}_{-0.38}$	$0.45^{+0.48\pm0.02}_{-0.41\pm0.01}$
Final spin a_f	$0.68^{+0.05}_{-0.07}$	$0.68^{+0.06}_{-0.05}$	$0.68^{+0.05\pm0.01}_{-0.06\pm0.02}$	$0.73^{+0.05}_{-0.06}$	$0.75^{+0.07}_{-0.05}$	$0.74^{+0.06\pm0.03}_{-0.06\pm0.03}$	$0.65^{+0.09}_{-0.10}$	$0.66^{+0.08}_{-0.10}$	$0.66^{+0.09\pm0.00}_{-0.10\pm0.02}$
Luminosity distance $D_\mathrm{L}/\mathrm{Mpc}$	400^{+160}_{-180}	440^{+140}_{-170}	$420^{+150\pm20}_{-180\pm40}$	450^{+180}_{-210}	440^{+170}_{-180}	$440^{+180\pm20}_{-190\pm10}$	1000^{+540}_{-490}	1030^{+480}_{-480}	$1020^{+500\pm20}_{-490\pm40}$
Source redshift z	$0.086^{+0.031}_{-0.036}$	$0.094^{+0.027}_{-0.034}$	$0.090^{+0.029\pm0.003}_{-0.036\pm0.008}$	$0.096^{+0.035}_{-0.042}$	$0.092^{+0.033}_{-0.037}$	$0.094^{+0.035\pm0.004}_{-0.039\pm0.001}$	$0.198^{+0.091}_{-0.092}$	$0.204^{+0.082}_{-0.088}$	$0.201^{+0.086\pm0.003}_{-0.091\pm0.008}$
Upper bound									
Primary spin magnitude a_1	0.62	0.73	0.67 ± 0.09	0.68	0.83	0.77 ± 0.12	0.64	0.69	0.67 ± 0.04
Secondary spin magnitude a_2	0.93	0.80	0.90 ± 0.12	0.90	0.89	0.90 ± 0.01	0.89	0.85	0.87 ± 0.04
Lower bound									
Mass ratio q	0.62	0.68	0.65 ± 0.05	0.25	0.30	0.28 ± 0.04	0.22	0.28	0.24 ± 0.05
Log Bayes factor $\ln \mathcal{B}_{\mathrm{s/n}}$	287.7 ± 0.1	289.8 ± 0.3	⋯	59.5 ± 0.1	60.2 ± 0.2	⋯	22.8 ± 0.2	23.0 ± 0.1	⋯
Information criterion DIC	32977.2 ± 0.3	32973.1 ± 0.1	⋯	34296.4 ± 0.2	34295.1 ± 0.1	⋯	94695.8 ± 0.0	94692.9 ± 0.0	⋯

M M_1 M_2 65 36 29 22 14 7.5

	GW150914			GW151226			LVT151012		
	EOBNR	IMRPhenom	Overall	EOBNR	IMRPhenom	Overall	EOBNR	IMRPhenom	Overall
Detector frame									
Total mass $M/\mathrm{M}_\odot$	$71.0^{+4.6}_{-4.0}$	$71.2^{+3.5}_{-3.2}$	$71.1^{+4.1\pm0.7}_{-3.6\pm0.8}$	$23.6^{+8.0}_{-1.3}$	$23.8^{+5.1}_{-1.5}$	$23.7^{+6.5\pm2.2}_{-1.4\pm0.1}$	45^{+17}_{-4}	44^{+12}_{-3}	$44^{+16\pm5}_{-3\pm0}$
Chirp mass $\mathcal{M}/\mathrm{M}_\odot$	$30.4^{+2.3}_{-1.6}$	$30.7^{+1.5}_{-1.5}$	$30.6^{+1.9\pm0.3}_{-1.6\pm0.4}$	$9.71^{+0.08}_{-0.07}$	$9.72^{+0.06}_{-0.06}$	$9.72^{+0.07\pm0.01}_{-0.06\pm0.01}$	$18.1^{+1.3}_{-0.9}$	$18.1^{+0.8}_{-0.8}$	$18.1^{+1.0\pm0.5}_{-0.8\pm0.1}$
Primary mass $m_1/\mathrm{M}_\odot$	$40.2^{+5.2}_{-4.8}$	$38.5^{+5.4}_{-3.3}$	$39.4^{+5.4\pm1.3}_{-4.1\pm0.2}$	$15.3^{+10.8}_{-3.8}$	$15.8^{+7.2}_{-4.0}$	$15.6^{+9.0\pm2.6}_{-4.0\pm0.2}$	29^{+23}_{-8}	27^{+19}_{-6}	$28^{+21\pm5}_{-7\pm0}$
Secondary mass $m_2/\mathrm{M}_\odot$	$30.6^{+5.1}_{-4.2}$	$32.7^{+3.1}_{-4.9}$	$31.7^{+4.0\pm0.1}_{-4.9\pm1.2}$	$8.3^{+2.5}_{-2.9}$	$8.1^{+2.5}_{-2.1}$	$8.2^{+2.6\pm0.2}_{-2.5\pm0.5}$	15^{+5}_{-6}	16^{+4}_{-6}	$16^{+5\pm0}_{-6\pm1}$
Final mass $M_\mathrm{f}/\mathrm{M}_\odot$	$67.8^{+4.0}_{-3.6}$	$67.9^{+3.2}_{-2.9}$	$67.8^{+3.7\pm0.6}_{-3.3\pm0.7}$	$22.5^{+8.2}_{-1.4}$	$22.8^{+5.3}_{-1.6}$	$22.6^{+6.7\pm2.2}_{-1.5\pm0.1}$	43^{+17}_{-4}	42^{+13}_{-2}	$42^{+16\pm5}_{-3\pm0}$
Source frame									
Total mass $M^\mathrm{source}/\mathrm{M}_\odot$	$65.5^{+4.4}_{-3.9}$	$65.1^{+3.6}_{-3.1}$	$65.3^{+4.1\pm1.0}_{-3.4\pm0.3}$	$21.6^{+7.4}_{-1.6}$	$21.9^{+4.7}_{-1.7}$	$21.8^{+5.9\pm2.0}_{-1.7\pm0.1}$	38^{+15}_{-5}	37^{+11}_{-4}	$37^{+13\pm4}_{-4\pm0}$
Chirp mass $\mathcal{M}^\mathrm{source}/\mathrm{M}_\odot$	$28.1^{+2.1}_{-1.6}$	$28.1^{+1.6}_{-1.4}$	$28.1^{+1.8\pm0.4}_{-1.5\pm0.2}$	$8.87^{+0.35}_{-0.28}$	$8.90^{+0.31}_{-0.27}$	$8.88^{+0.33\pm0.01}_{-0.28\pm0.04}$	$15.2^{+1.5}_{-1.1}$	$15.0^{+1.3}_{-1.0}$	$15.1^{+1.4\pm0.3}_{-1.1\pm0.0}$
Primary mass $m_1^\mathrm{source}/\mathrm{M}_\odot$	$37.0^{+4.9}_{-4.4}$	$35.3^{+5.1}_{-3.1}$	$36.2^{+5.2\pm1.4}_{-3.8\pm0.4}$	$14.0^{+10.0}_{-3.5}$	$14.5^{+6.6}_{-3.7}$	$14.2^{+8.3\pm2.4}_{-3.7\pm0.2}$	24^{+19}_{-7}	23^{+16}_{-5}	$23^{+18\pm5}_{-6\pm0}$
Secondary mass $m_2^\mathrm{source}/\mathrm{M}_\odot$	$28.3^{+4.6}_{-3.9}$	$29.9^{+3.0}_{-4.5}$	$29.1^{+3.7\pm0.0}_{-4.4\pm0.9}$	$7.5^{+2.3}_{-2.6}$	$7.4^{+2.3}_{-2.0}$	$7.5^{+2.3\pm0.2}_{-2.3\pm0.4}$	13^{+4}_{-5}	14^{+4}_{-5}	$13^{+4\pm0}_{-5\pm0}$
Final mass $M_\mathrm{f}^\mathrm{source}/\mathrm{M}_\odot$	$62.5^{+3.9}_{-3.5}$	$62.1^{+3.3}_{-2.8}$	$62.3^{+3.7\pm0.9}_{-3.1\pm0.2}$	$20.6^{+7.6}_{-1.6}$	$20.9^{+4.8}_{-1.8}$	$20.8^{+6.1\pm2.0}_{-1.7\pm0.1}$	36^{+15}_{-4}	35^{+11}_{-3}	$35^{+14\pm4}_{-4\pm0}$
Energy radiated $E_\mathrm{rad}/(\mathrm{M}_\odot c^2)$	$2.98^{+0.55}_{-0.40}$	$3.02^{+0.36}_{-0.36}$	$3.00^{+0.47\pm0.13}_{-0.39\pm0.07}$	$1.02^{+0.09}_{-0.24}$	$0.99^{+0.11}_{-0.17}$	$1.00^{+0.10\pm0.01}_{-0.20\pm0.03}$	$1.48^{+0.39}_{-0.41}$	$1.51^{+0.29}_{-0.44}$	$1.50^{+0.33\pm0.05}_{-0.43\pm0.01}$
Mass ratio q	$0.77^{+0.20}_{-0.18}$	$0.85^{+0.13}_{-0.21}$	$0.81^{+0.17\pm0.02}_{-0.20\pm0.04}$	$0.54^{+0.40}_{-0.33}$	$0.51^{+0.39}_{-0.25}$	$0.52^{+0.40\pm0.03}_{-0.29\pm0.04}$	$0.53^{+0.42}_{-0.34}$	$0.60^{+0.35}_{-0.37}$	$0.57^{+0.38\pm0.01}_{-0.37\pm0.04}$
Effective inspiral spin χ_eff	$-0.08^{+0.17}_{-0.14}$	$-0.05^{+0.11}_{-0.12}$	$-0.06^{+0.14\pm0.02}_{-0.14\pm0.04}$	$0.21^{+0.24}_{-0.11}$	$0.22^{+0.15}_{-0.08}$	$0.21^{+0.20\pm0.07}_{-0.10\pm0.03}$	$0.06^{+0.31}_{-0.24}$	$0.01^{+0.26}_{-0.17}$	$0.03^{+0.31\pm0.08}_{-0.20\pm0.02}$
Primary spin magnitude a_1	$0.33^{+0.39}_{-0.29}$	$0.30^{+0.54}_{-0.27}$	$0.32^{+0.47\pm0.10}_{-0.29\pm0.01}$	$0.42^{+0.35}_{-0.37}$	$0.55^{+0.35}_{-0.42}$	$0.49^{+0.37\pm0.11}_{-0.42\pm0.07}$	$0.31^{+0.46}_{-0.27}$	$0.31^{+0.50}_{-0.28}$	$0.31^{+0.48\pm0.03}_{-0.28\pm0.00}$
Secondary spin magnitude a_2	$0.62^{+0.35}_{-0.54}$	$0.36^{+0.53}_{-0.33}$	$0.48^{+0.47\pm0.08}_{-0.43\pm0.03}$	$0.51^{+0.44}_{-0.46}$	$0.52^{+0.42}_{-0.47}$	$0.52^{+0.43\pm0.01}_{-0.47\pm0.00}$	$0.49^{+0.45}_{-0.44}$	$0.42^{+0.50}_{-0.38}$	$0.45^{+0.48\pm0.02}_{-0.41\pm0.01}$
Final spin a_f	$0.68^{+0.05}_{-0.07}$	$0.68^{+0.06}_{-0.05}$	$0.68^{+0.05\pm0.01}_{-0.06\pm0.02}$	$0.73^{+0.05}_{-0.06}$	$0.75^{+0.07}_{-0.05}$	$0.74^{+0.06\pm0.03}_{-0.06\pm0.03}$	$0.65^{+0.09}_{-0.10}$	$0.66^{+0.08}_{-0.10}$	$0.66^{+0.09\pm0.00}_{-0.10\pm0.02}$
Luminosity distance $D_\mathrm{L}/\mathrm{Mpc}$	400^{+160}_{-180}	440^{+140}_{-170}	$420^{+150\pm20}_{-180\pm40}$	450^{+180}_{-210}	440^{+170}_{-180}	$440^{+180\pm20}_{-190\pm10}$	1000^{+540}_{-490}	1030^{+480}_{-480}	$1020^{+500\pm20}_{-490\pm40}$
Source redshift z	$0.086^{+0.031}_{-0.036}$	$0.094^{+0.027}_{-0.034}$	$0.090^{+0.029\pm0.003}_{-0.036\pm0.008}$	$0.096^{+0.035}_{-0.042}$	$0.092^{+0.033}_{-0.037}$	$0.094^{+0.035\pm0.004}_{-0.039\pm0.001}$	$0.198^{+0.091}_{-0.092}$	$0.204^{+0.082}_{-0.088}$	$0.201^{+0.086\pm0.003}_{-0.091\pm0.008}$
Upper bound									
Primary spin magnitude a_1	0.62	0.73	0.67 ± 0.09	0.68	0.83	0.77 ± 0.12	0.64	0.69	0.67 ± 0.04
Secondary spin magnitude a_2	0.93	0.80	0.90 ± 0.12	0.90	0.89	0.90 ± 0.01	0.89	0.85	0.87 ± 0.04
Lower bound									
Mass ratio q	0.62	0.68	0.65 ± 0.05	0.25	0.30	0.28 ± 0.04	0.22	0.28	0.24 ± 0.05
Log Bayes factor $\ln \mathcal{B}_{\mathrm{s/n}}$	287.7 ± 0.1	289.8 ± 0.3	⋯	59.5 ± 0.1	60.2 ± 0.2	⋯	22.8 ± 0.2	23.0 ± 0.1	⋯
Information criterion DIC	32977.2 ± 0.3	32973.1 ± 0.1	⋯	34296.4 ± 0.2	34295.1 ± 0.1	⋯	94695.8 ± 0.0	94692.9 ± 0.0	⋯

M M_1 M_2 65 36 29 22 14 7.5 37 23 13

	GW150914			GW151226			LVT151012		
	EOBNR	IMRPhenom	Overall	EOBNR	IMRPhenom	Overall	EOBNR	IMRPhenom	Overall
Detector frame									
Total mass $M/\mathrm{M}_\odot$	$71.0^{+4.6}_{-4.0}$	$71.2^{+3.5}_{-3.2}$	$71.1^{+4.1\pm0.7}_{-3.6\pm0.8}$	$23.6^{+8.0}_{-1.3}$	$23.8^{+5.1}_{-1.5}$	$23.7^{+6.5\pm2.2}_{-1.4\pm0.1}$	45^{+17}_{-4}	44^{+12}_{-3}	$44^{+16\pm5}_{-3\pm0}$
Chirp mass $\mathcal{M}/\mathrm{M}_\odot$	$30.4^{+2.3}_{-1.6}$	$30.7^{+1.5}_{-1.5}$	$30.6^{+1.9\pm0.3}_{-1.6\pm0.4}$	$9.71^{+0.08}_{-0.07}$	$9.72^{+0.06}_{-0.06}$	$9.72^{+0.07\pm0.01}_{-0.06\pm0.01}$	$18.1^{+1.3}_{-0.9}$	$18.1^{+0.8}_{-0.8}$	$18.1^{+1.0\pm0.5}_{-0.8\pm0.1}$
Primary mass $m_1/\mathrm{M}_\odot$	$40.2^{+5.2}_{-4.8}$	$38.5^{+5.4}_{-3.3}$	$39.4^{+5.4\pm1.3}_{-4.1\pm0.2}$	$15.3^{+10.8}_{-3.8}$	$15.8^{+7.2}_{-4.0}$	$15.6^{+9.0\pm2.6}_{-4.0\pm0.2}$	29^{+23}_{-8}	27^{+19}_{-6}	$28^{+21\pm5}_{-7\pm0}$
Secondary mass $m_2/\mathrm{M}_\odot$	$30.6^{+5.1}_{-4.2}$	$32.7^{+3.1}_{-4.9}$	$31.7^{+4.0\pm0.1}_{-4.9\pm1.2}$	$8.3^{+2.5}_{-2.9}$	$8.1^{+2.5}_{-2.1}$	$8.2^{+2.6\pm0.2}_{-2.5\pm0.5}$	15^{+5}_{-6}	16^{+4}_{-6}	$16^{+5\pm0}_{-6\pm1}$
Final mass $M_\mathrm{f}/\mathrm{M}_\odot$	$67.8^{+4.0}_{-3.6}$	$67.9^{+3.2}_{-2.9}$	$67.8^{+3.7\pm0.6}_{-3.3\pm0.7}$	$22.5^{+8.2}_{-1.4}$	$22.8^{+5.3}_{-1.6}$	$22.6^{+6.7\pm2.2}_{-1.5\pm0.1}$	43^{+17}_{-4}	42^{+13}_{-2}	$42^{+16\pm5}_{-3\pm0}$
Source frame									
Total mass $M^\mathrm{source}/\mathrm{M}_\odot$	$65.5^{+4.4}_{-3.9}$	$65.1^{+3.6}_{-3.1}$	$65.3^{+4.1\pm1.0}_{-3.4\pm0.3}$	$21.6^{+7.4}_{-1.6}$	$21.9^{+4.7}_{-1.7}$	$21.8^{+5.9\pm2.0}_{-1.7\pm0.1}$	38^{+15}_{-5}	37^{+11}_{-4}	$37^{+13\pm4}_{-4\pm0}$
Chirp mass $\mathcal{M}^\mathrm{source}/\mathrm{M}_\odot$	$28.1^{+2.1}_{-1.6}$	$28.1^{+1.6}_{-1.4}$	$28.1^{+1.8\pm0.4}_{-1.5\pm0.2}$	$8.87^{+0.35}_{-0.28}$	$8.90^{+0.31}_{-0.27}$	$8.88^{+0.33\pm0.01}_{-0.28\pm0.04}$	$15.2^{+1.5}_{-1.1}$	$15.0^{+1.3}_{-1.0}$	$15.1^{+1.4\pm0.3}_{-1.1\pm0.0}$
Primary mass $m_1^\mathrm{source}/\mathrm{M}_\odot$	$37.0^{+4.9}_{-4.4}$	$35.3^{+5.1}_{-3.1}$	$36.2^{+5.2\pm1.4}_{-3.8\pm0.4}$	$14.0^{+10.0}_{-3.5}$	$14.5^{+6.6}_{-3.7}$	$14.2^{+8.3\pm2.4}_{-3.7\pm0.2}$	24^{+19}_{-7}	23^{+16}_{-5}	$23^{+18\pm5}_{-6\pm0}$
Secondary mass $m_2^\mathrm{source}/\mathrm{M}_\odot$	$28.3^{+4.6}_{-3.9}$	$29.9^{+3.0}_{-4.5}$	$29.1^{+3.7\pm0.0}_{-4.4\pm0.9}$	$7.5^{+2.3}_{-2.6}$	$7.4^{+2.3}_{-2.0}$	$7.5^{+2.3\pm0.2}_{-2.3\pm0.4}$	13^{+4}_{-5}	14^{+4}_{-5}	$13^{+4\pm0}_{-5\pm0}$
Final mass $M_\mathrm{f}^\mathrm{source}/\mathrm{M}_\odot$	$62.5^{+3.9}_{-3.5}$	$62.1^{+3.3}_{-2.8}$	$62.3^{+3.7\pm0.9}_{-3.1\pm0.2}$	$20.6^{+7.6}_{-1.6}$	$20.9^{+4.8}_{-1.8}$	$20.8^{+6.1\pm2.0}_{-1.7\pm0.1}$	36^{+15}_{-4}	35^{+11}_{-3}	$35^{+14\pm4}_{-4\pm0}$
Energy radiated $E_\mathrm{rad}/(\mathrm{M}_\odot c^2)$	$2.98^{+0.55}_{-0.40}$	$3.02^{+0.36}_{-0.36}$	$3.00^{+0.47\pm0.13}_{-0.39\pm0.07}$	$1.02^{+0.09}_{-0.24}$	$0.99^{+0.11}_{-0.17}$	$1.00^{+0.10\pm0.01}_{-0.20\pm0.03}$	$1.48^{+0.39}_{-0.41}$	$1.51^{+0.29}_{-0.44}$	$1.50^{+0.33\pm0.05}_{-0.43\pm0.01}$
Mass ratio q	$0.77^{+0.20}_{-0.18}$	$0.85^{+0.13}_{-0.21}$	$0.81^{+0.17\pm0.02}_{-0.20\pm0.04}$	$0.54^{+0.40}_{-0.33}$	$0.51^{+0.39}_{-0.25}$	$0.52^{+0.40\pm0.03}_{-0.29\pm0.04}$	$0.53^{+0.42}_{-0.34}$	$0.60^{+0.35}_{-0.37}$	$0.57^{+0.38\pm0.01}_{-0.37\pm0.04}$
Effective inspiral spin χ_eff	$-0.08^{+0.17}_{-0.14}$	$-0.05^{+0.11}_{-0.12}$	$-0.06^{+0.14\pm0.02}_{-0.14\pm0.04}$	$0.21^{+0.24}_{-0.11}$	$0.22^{+0.15}_{-0.08}$	$0.21^{+0.20\pm0.07}_{-0.10\pm0.03}$	$0.06^{+0.31}_{-0.24}$	$0.01^{+0.26}_{-0.17}$	$0.03^{+0.31\pm0.08}_{-0.20\pm0.02}$
Primary spin magnitude a_1	$0.33^{+0.39}_{-0.29}$	$0.30^{+0.54}_{-0.27}$	$0.32^{+0.47\pm0.10}_{-0.29\pm0.01}$	$0.42^{+0.35}_{-0.37}$	$0.55^{+0.35}_{-0.42}$	$0.49^{+0.37\pm0.11}_{-0.42\pm0.07}$	$0.31^{+0.46}_{-0.27}$	$0.31^{+0.50}_{-0.28}$	$0.31^{+0.48\pm0.03}_{-0.28\pm0.00}$
Secondary spin magnitude a_2	$0.62^{+0.35}_{-0.54}$	$0.36^{+0.53}_{-0.33}$	$0.48^{+0.47\pm0.08}_{-0.43\pm0.03}$	$0.51^{+0.44}_{-0.46}$	$0.52^{+0.42}_{-0.47}$	$0.52^{+0.43\pm0.01}_{-0.47\pm0.00}$	$0.49^{+0.45}_{-0.44}$	$0.42^{+0.50}_{-0.38}$	$0.45^{+0.48\pm0.02}_{-0.41\pm0.01}$
Final spin a_f	$0.68^{+0.05}_{-0.07}$	$0.68^{+0.06}_{-0.05}$	$0.68^{+0.05\pm0.01}_{-0.06\pm0.02}$	$0.73^{+0.05}_{-0.06}$	$0.75^{+0.07}_{-0.05}$	$0.74^{+0.06\pm0.03}_{-0.06\pm0.03}$	$0.65^{+0.09}_{-0.10}$	$0.66^{+0.08}_{-0.10}$	$0.66^{+0.09\pm0.00}_{-0.10\pm0.02}$
Luminosity distance $D_\mathrm{L}/\mathrm{Mpc}$	400^{+160}_{-180}	440^{+140}_{-170}	$420^{+150\pm20}_{-180\pm40}$	450^{+180}_{-210}	440^{+170}_{-180}	$440^{+180\pm20}_{-190\pm10}$	1000^{+540}_{-490}	1030^{+480}_{-480}	$1020^{+500\pm20}_{-490\pm40}$
Source redshift z	$0.086^{+0.031}_{-0.036}$	$0.094^{+0.027}_{-0.034}$	$0.090^{+0.029\pm0.003}_{-0.036\pm0.008}$	$0.096^{+0.035}_{-0.042}$	$0.092^{+0.033}_{-0.037}$	$0.094^{+0.035\pm0.004}_{-0.039\pm0.001}$	$0.198^{+0.091}_{-0.092}$	$0.204^{+0.082}_{-0.088}$	$0.201^{+0.086\pm0.003}_{-0.091\pm0.008}$
Upper bound									
Primary spin magnitude a_1	0.62	0.73	0.67 ± 0.09	0.68	0.83	0.77 ± 0.12	0.64	0.69	0.67 ± 0.04
Secondary spin magnitude a_2	0.93	0.80	0.90 ± 0.12	0.90	0.89	0.90 ± 0.01	0.89	0.85	0.87 ± 0.04
Lower bound									
Mass ratio q	0.62	0.68	0.65 ± 0.05	0.25	0.30	0.28 ± 0.04	0.22	0.28	0.24 ± 0.05
Log Bayes factor $\ln \mathcal{B}_{\mathrm{s/n}}$	287.7 ± 0.1	289.8 ± 0.3	⋯	59.5 ± 0.1	60.2 ± 0.2	⋯	22.8 ± 0.2	23.0 ± 0.1	⋯
Information criterion DIC	32977.2 ± 0.3	32973.1 ± 0.1	⋯	34296.4 ± 0.2	34295.1 ± 0.1	⋯	94695.8 ± 0.0	94692.9 ± 0.0	⋯

Outline

- Gravitational radiation emission from the source.
- Gravitational radiation detection from interferometers.
- Parameter estimation.
- Event rates and formation scenarios.

Emission from the source

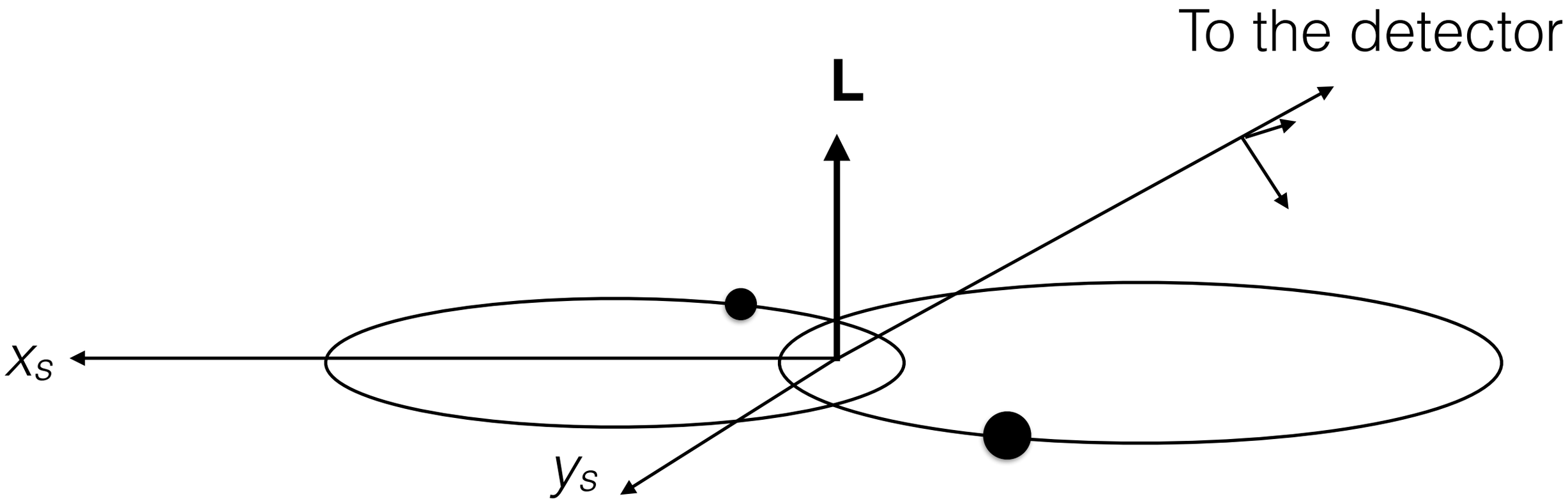

Emission from the source

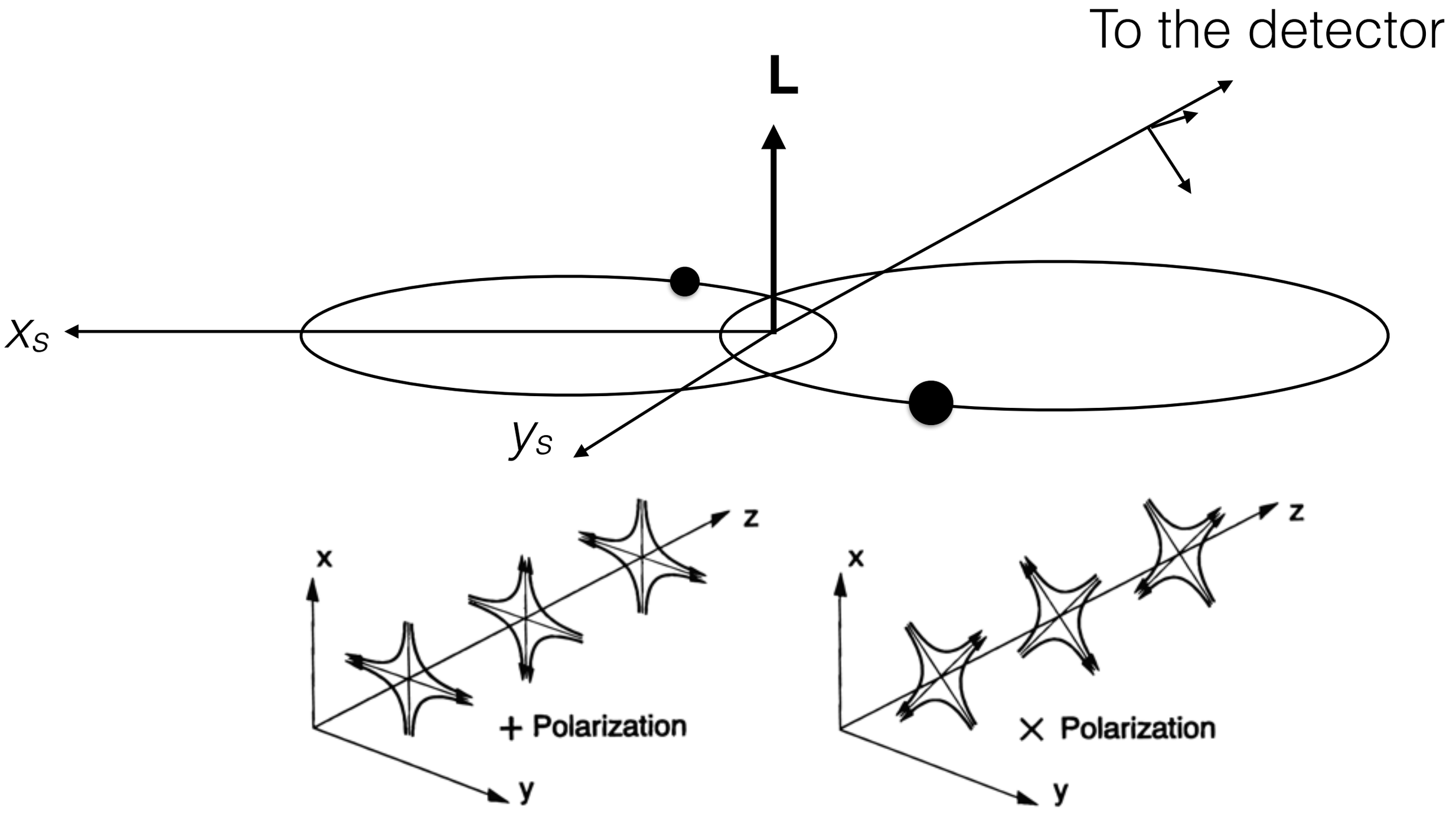

+ X

e = 0

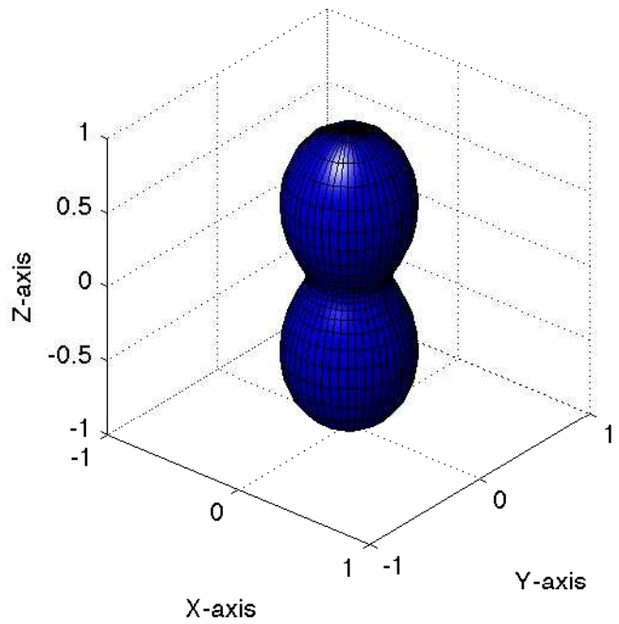
Z-axis
1
0.5
0
-0.5
-1
-1
0
1
X-axis
1
0
-1
Y-axis

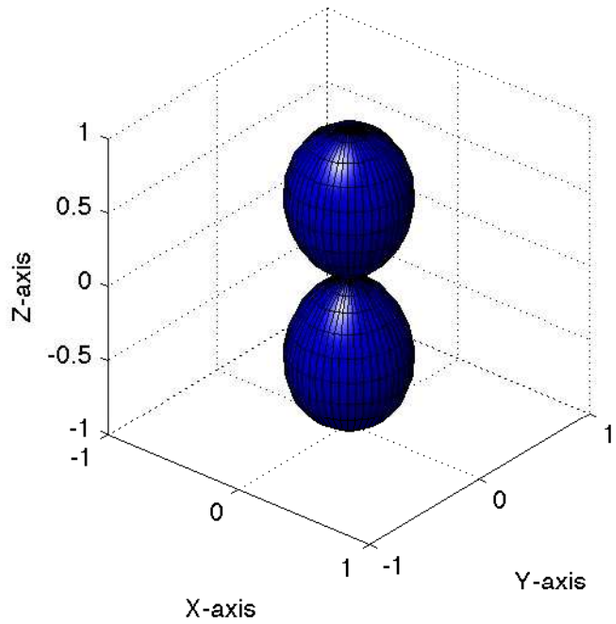
Z-axis
1
0.5
0
-0.5
-1
-1
0
1
X-axis
1
0
-1
Y-axis

e = 0.999

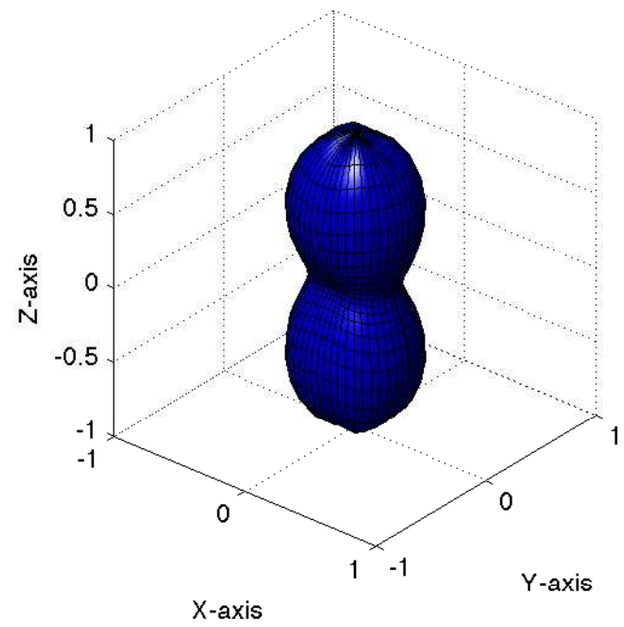
Z-axis
1
0.5
0
-0.5
-1
-1
0
1
X-axis
1
0
-1
Y-axis

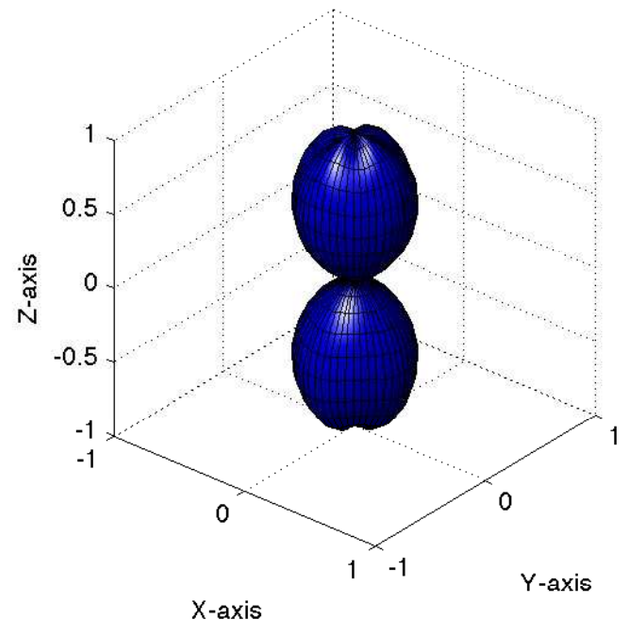
Z-axis
1
0.5
0
-0.5
-1
-1
0
1
X-axis
1
0
-1
Y-axis

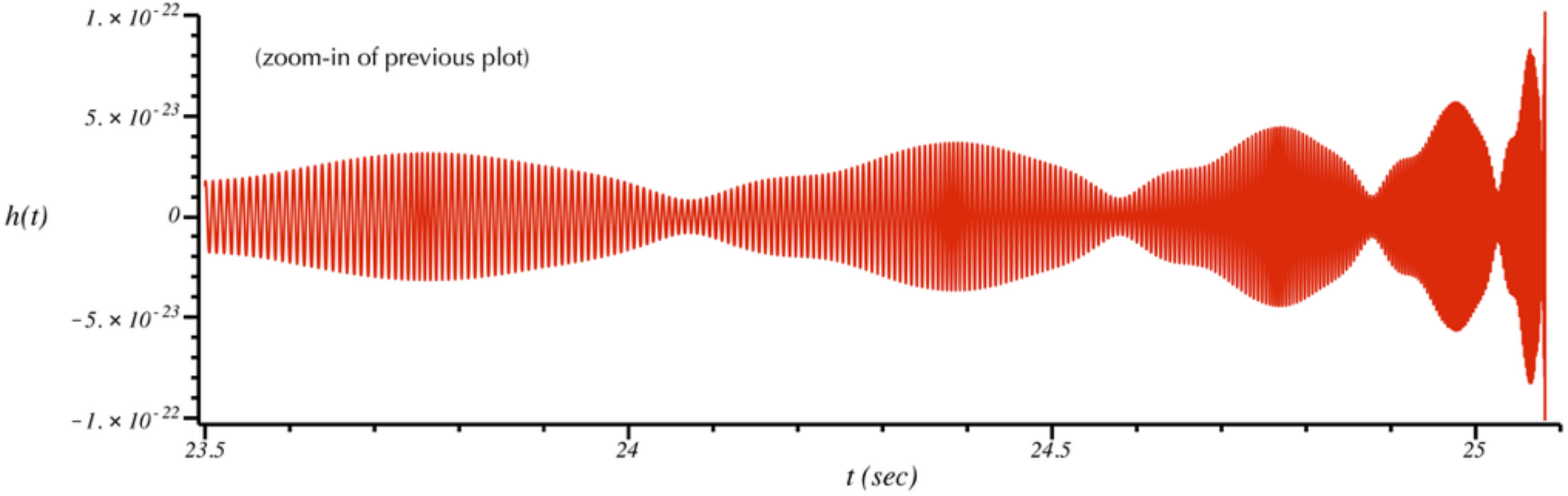

http://www.soundsofspacetime.org/spinning-binaries.html

Can measure initial spins through spin-orbit coupling if enough cycles of inspiral are measured.

Interferometric Detection

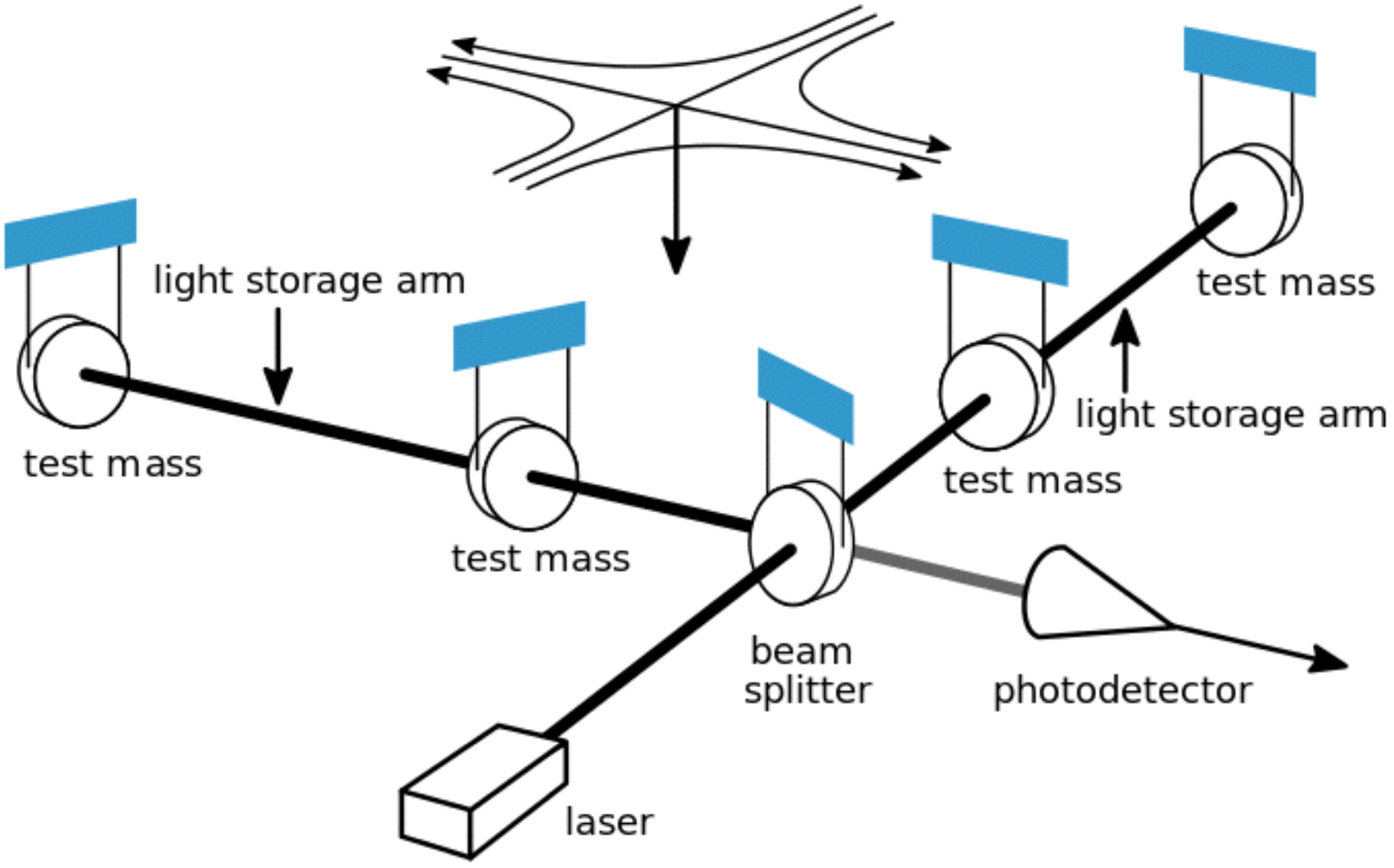

"+" pattern, ψ=0

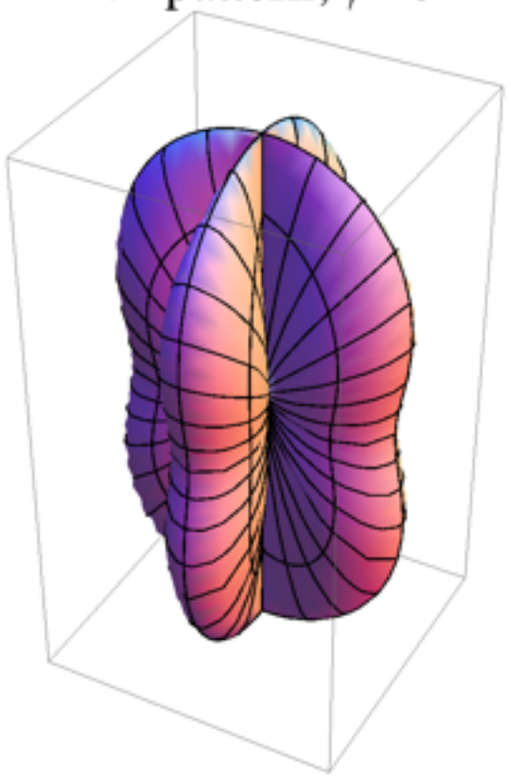

"×" pattern, ψ=π/4

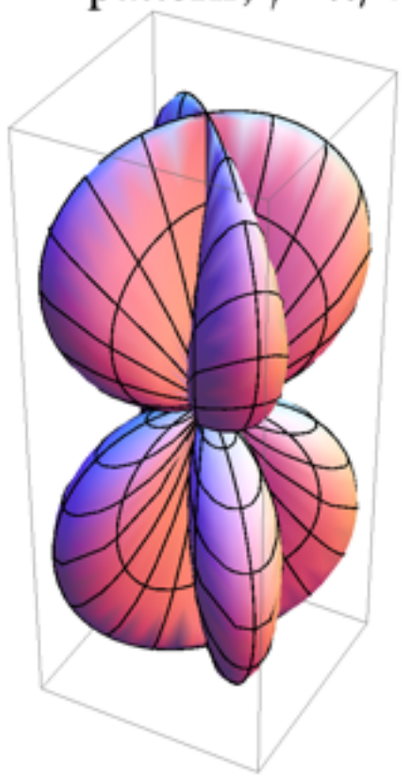

RMS antenna pattern

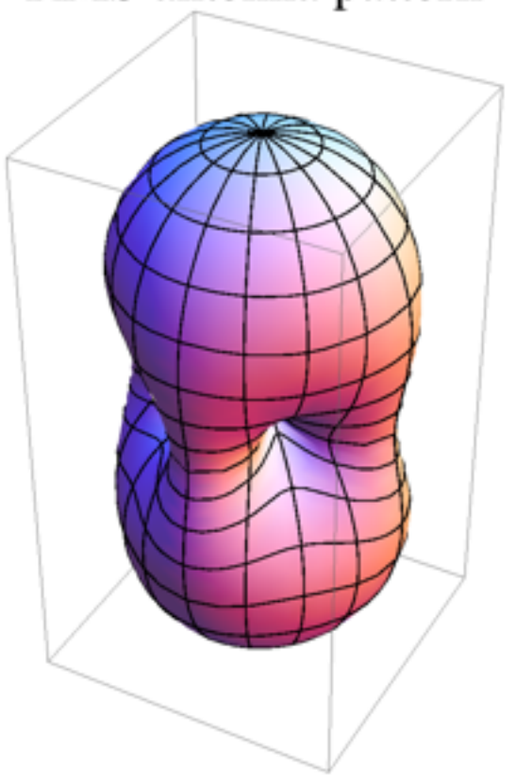

Parameter estimation

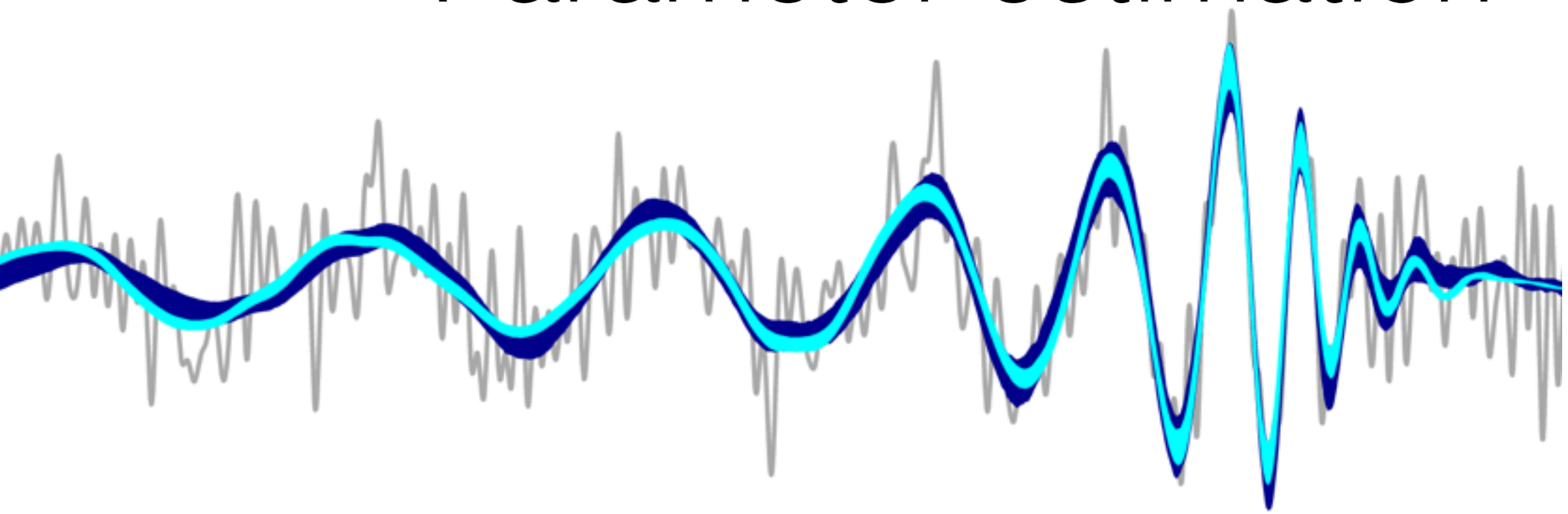

Inspiral Merger Ringdown

Newtonian → PN → NR → Perturbation

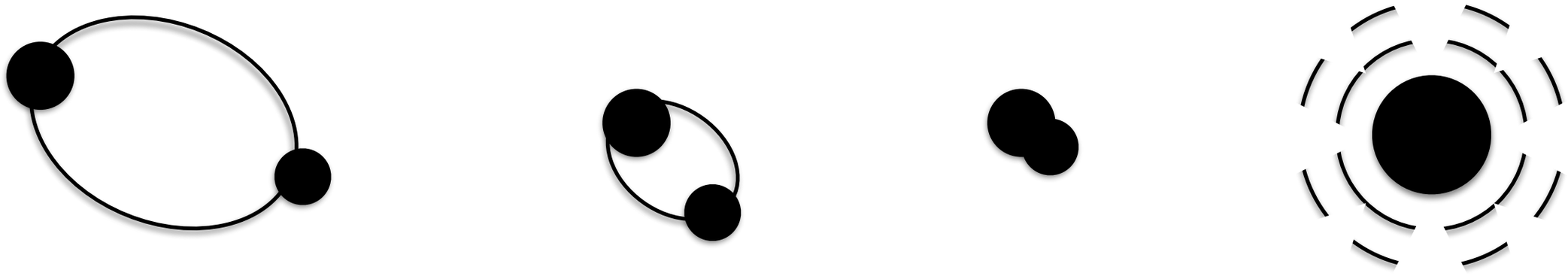

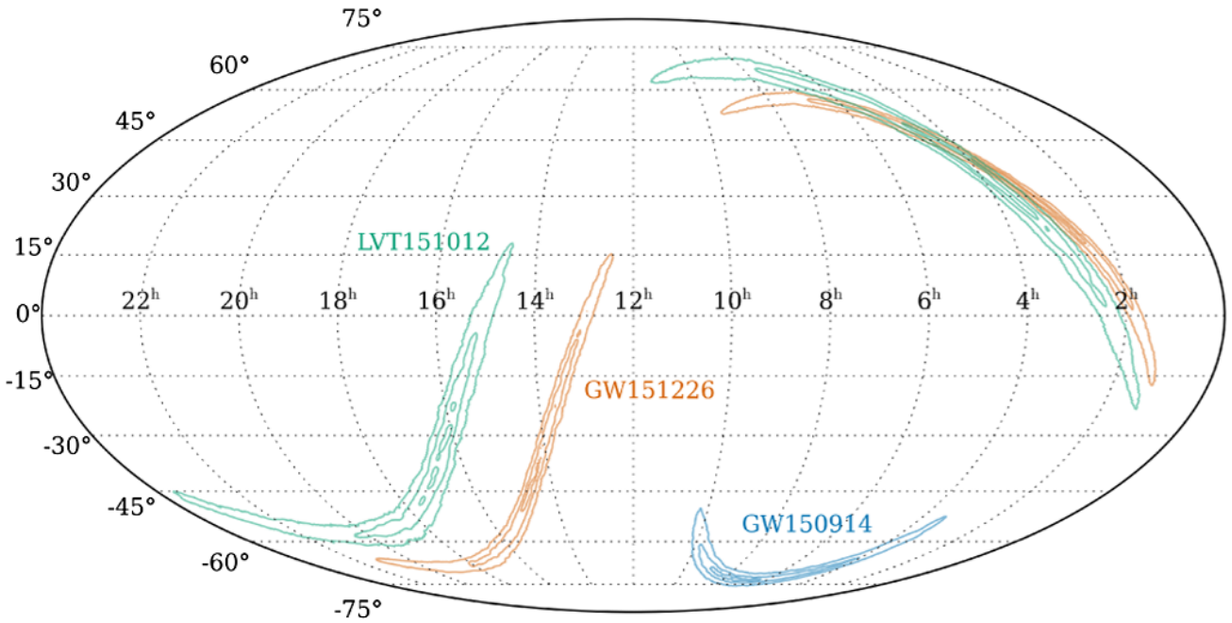
75°
60°
45°
30°
15°
0°
-15°
-30°
-45°
-60°
-75°
22h
20h
18h
16h
14h
12h
10h
8h
6h
4h
2h
LVT151012
GW151226
GW150914

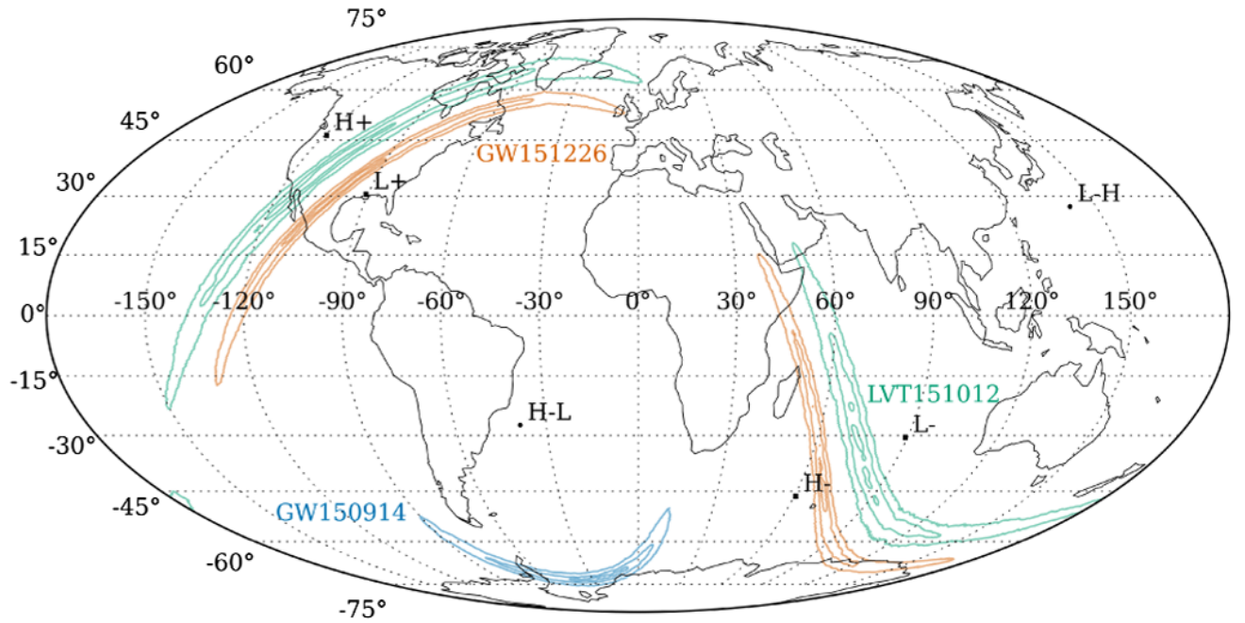
75°
60°
45°
30°
15°
0°
-15°
-30°
-45°
-60°
-75°
-150°
-120°
-90°
-60°
-30°
0°
30°
60°
90°
120°
150°
H+
L+
H-L
L-H
H-
L-
GW151226
LVT151012
GW150914

$$\mathcal{M}_c = \mu^{3/5} M^{2/5}$$

$$\frac{v^2}{c^2} \quad \text{and} \quad \frac{G\mu M}{rc^2}$$

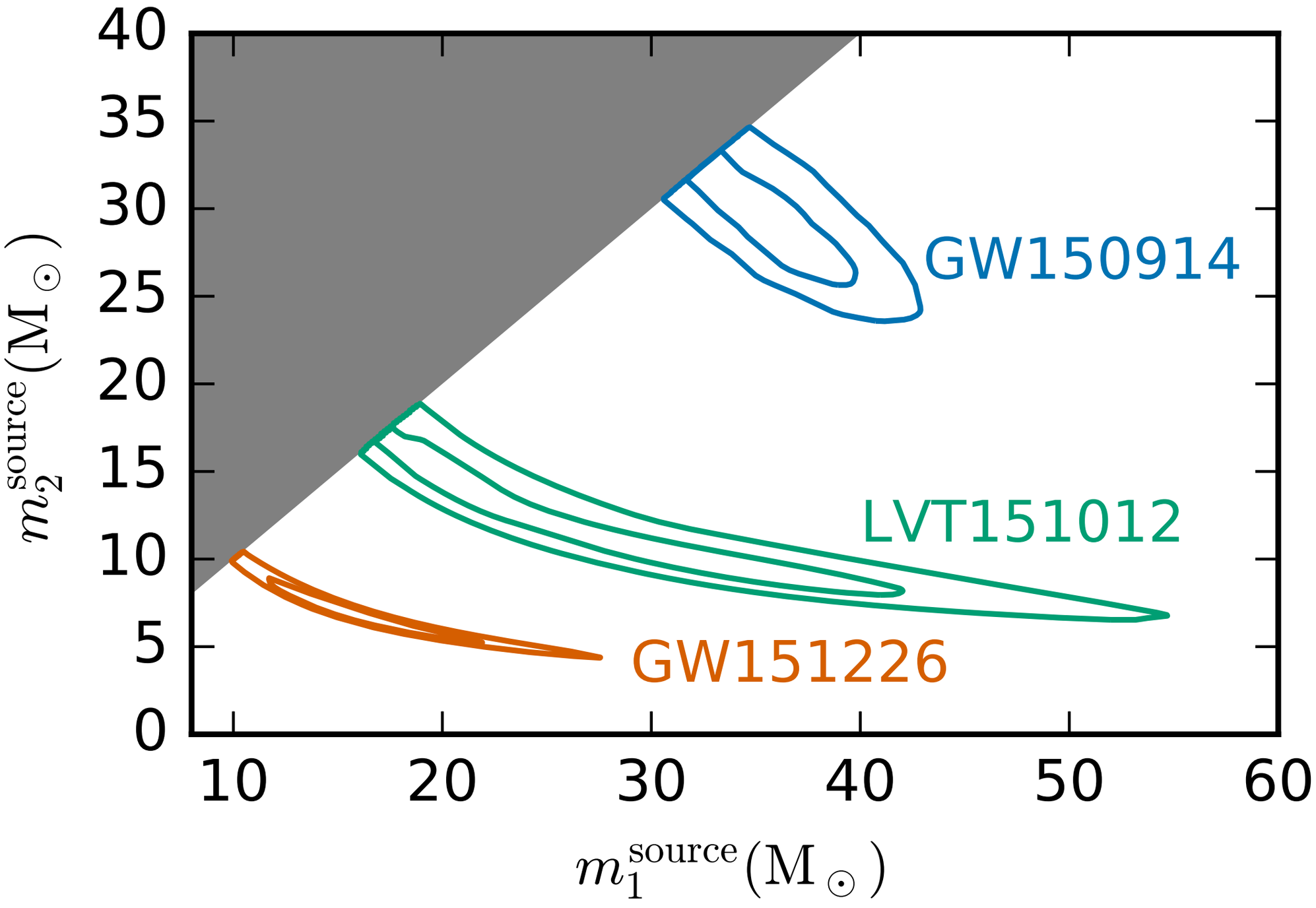

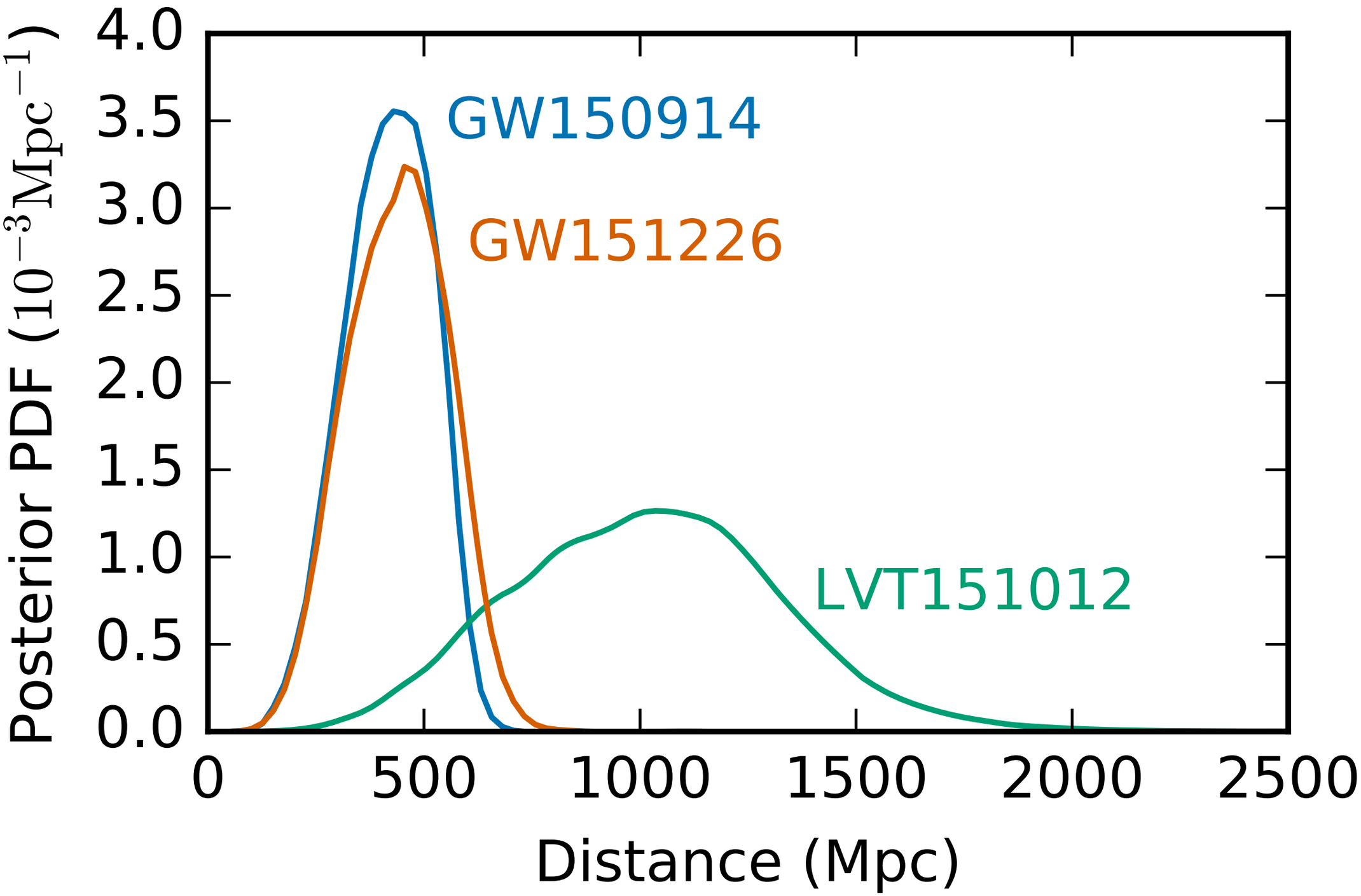
GW150914
GW151226
LVT151012
Posterior PDF (10^{-3}Mpc^{-1})
4.0
3.5
3.0
2.5
2.0
1.5
1.0
0.5
0.0
0
500
1000
1500
2000
2500
Distance (Mpc)

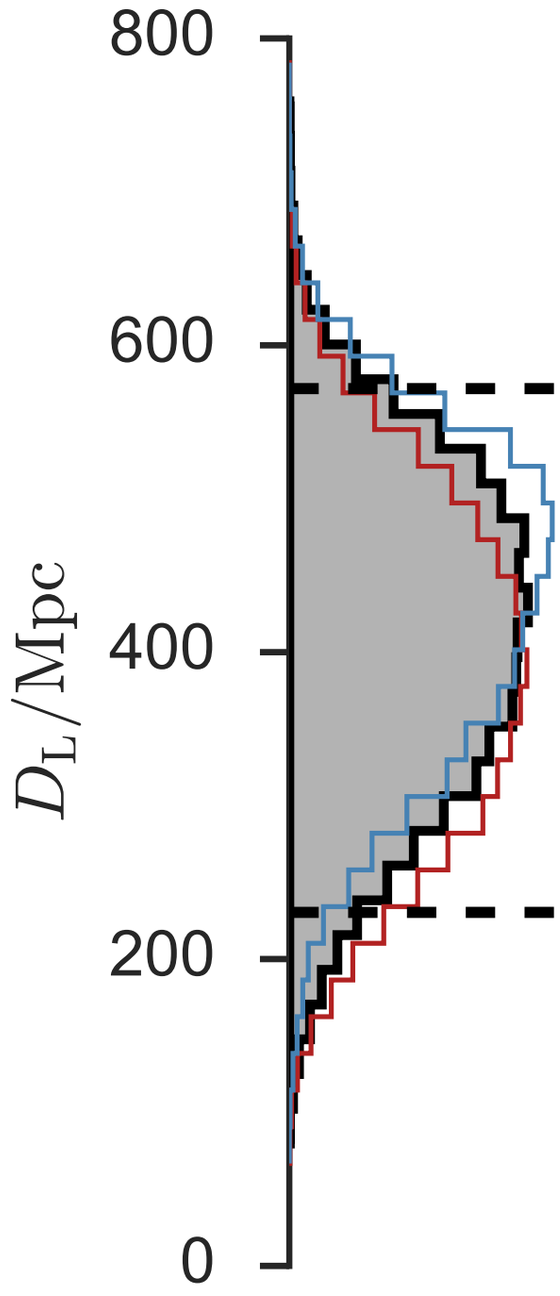

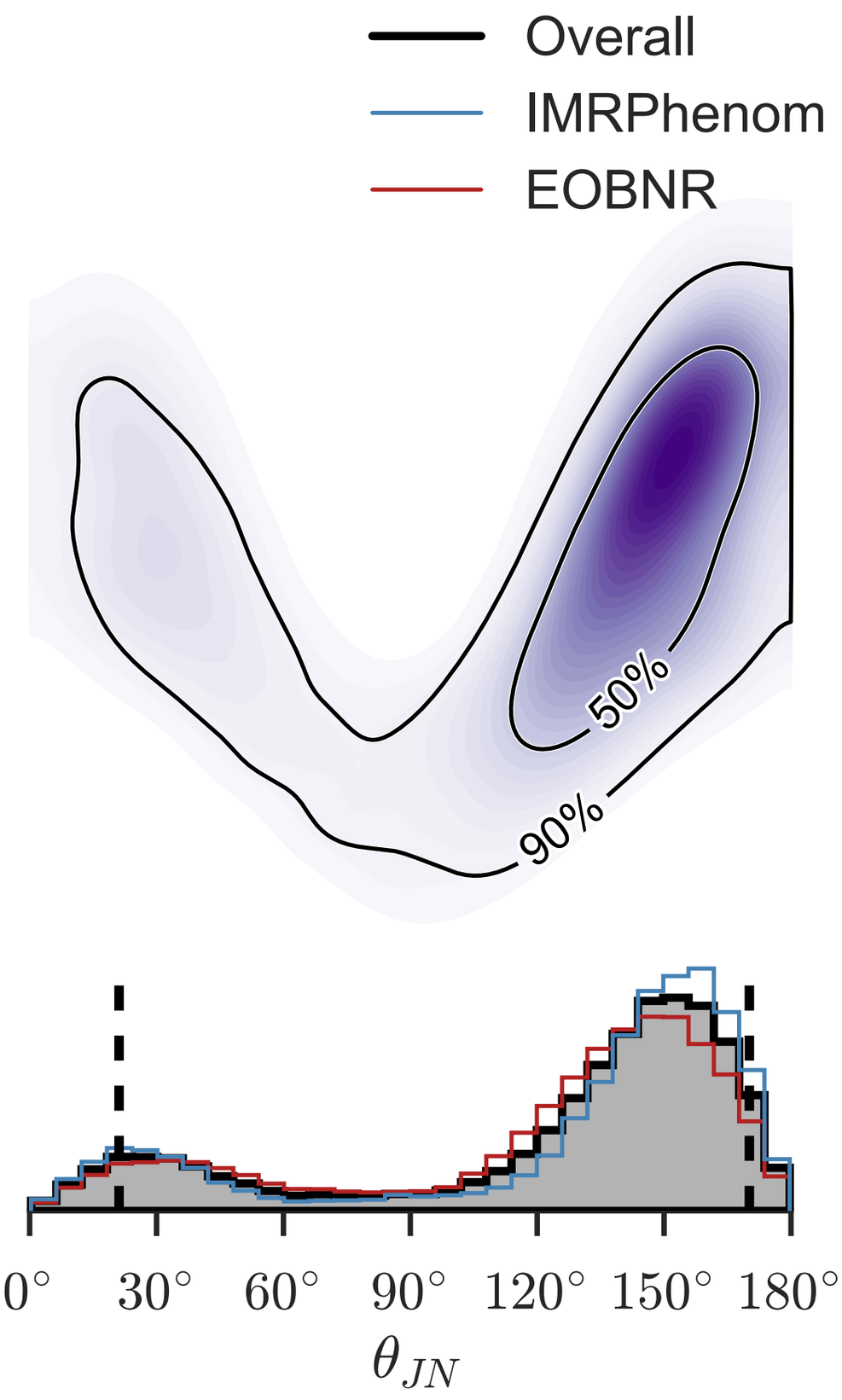

$$D_{\rm L} \propto \frac{\dot{f}}{hf^3}$$

Histogram of Inclinations

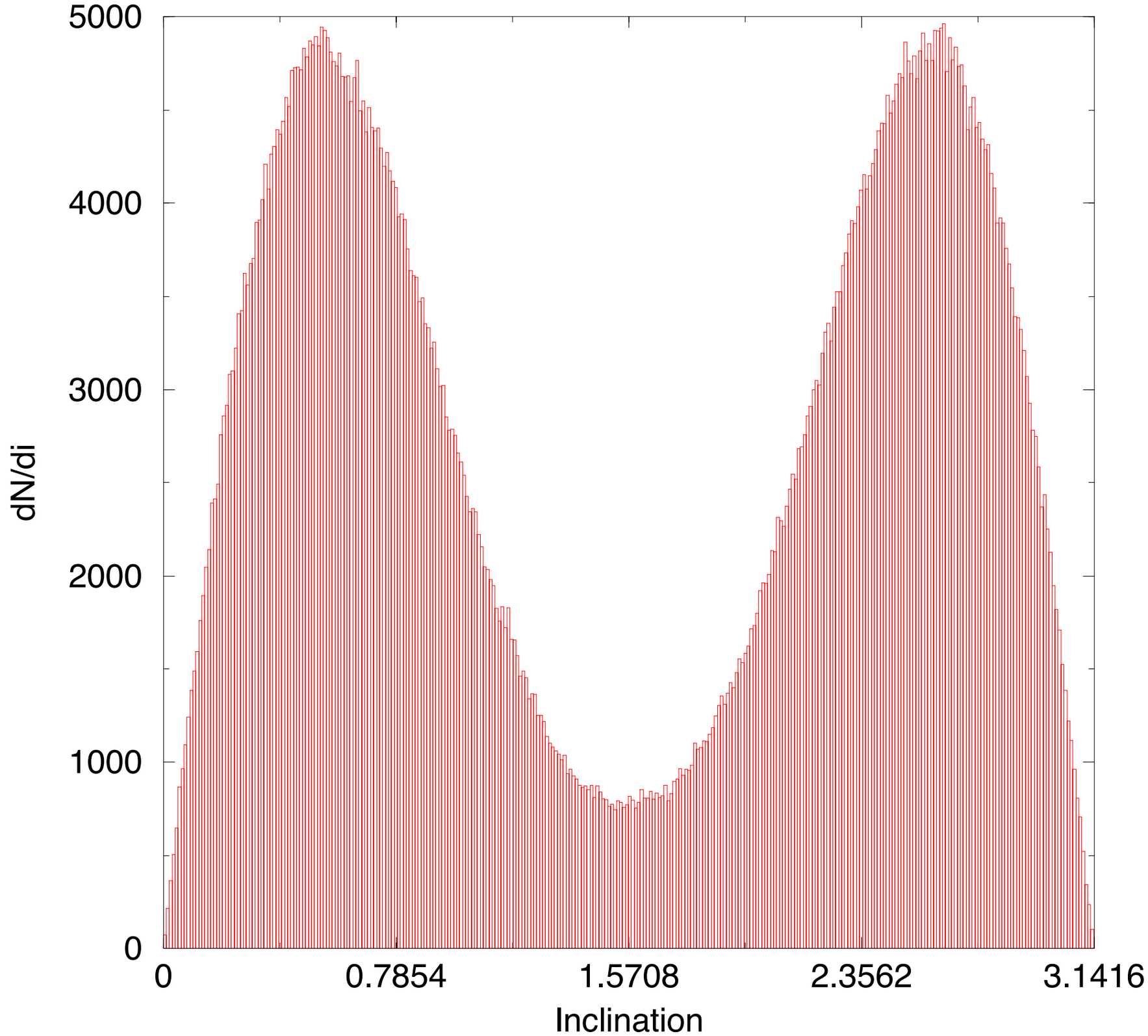

$$f \simeq 32\,\mathrm{kHz} \times \left(1 - 0.63\,(1-a)^{0.3}\right)\left(\frac{M_\odot}{M}\right)$$

$$Q \simeq 2\,(1-a)^{-0.45}$$

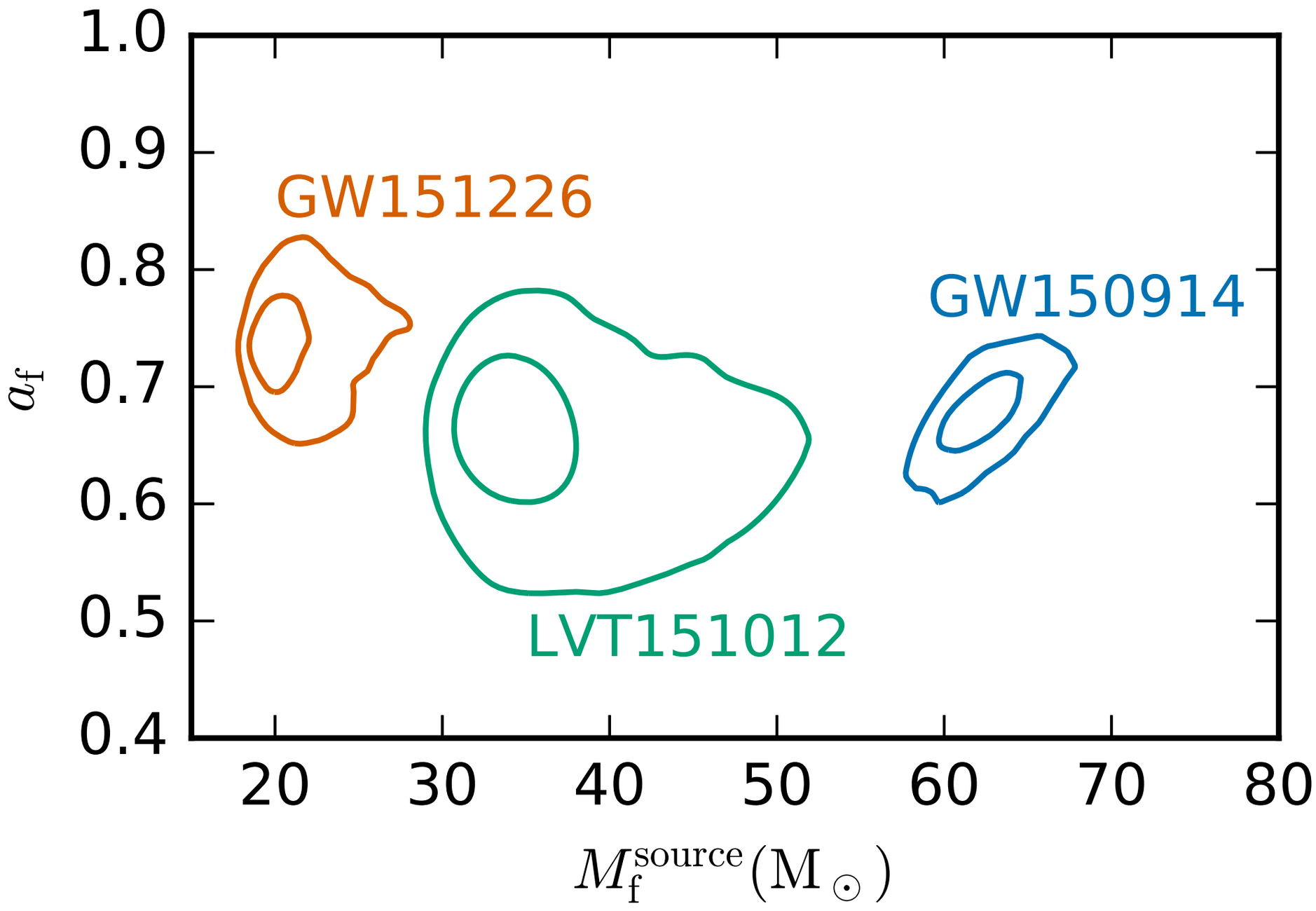

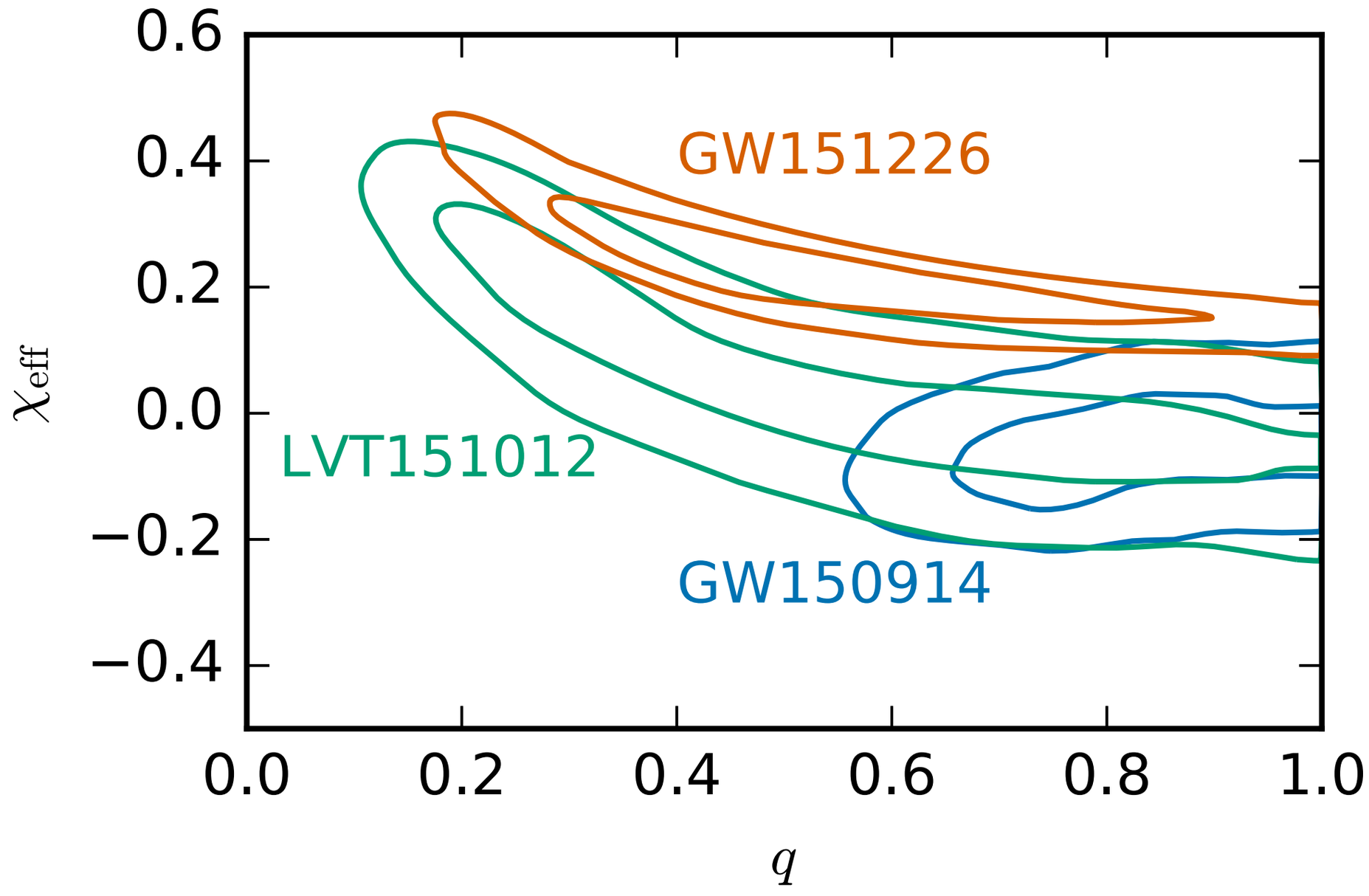
0.6
0.4
0.2
0.0
−0.2
−0.4
$\chi_{\rm eff}$
GW151226
LVT151012
GW150914
0.0
0.2
0.4
0.6
0.8
1.0
q

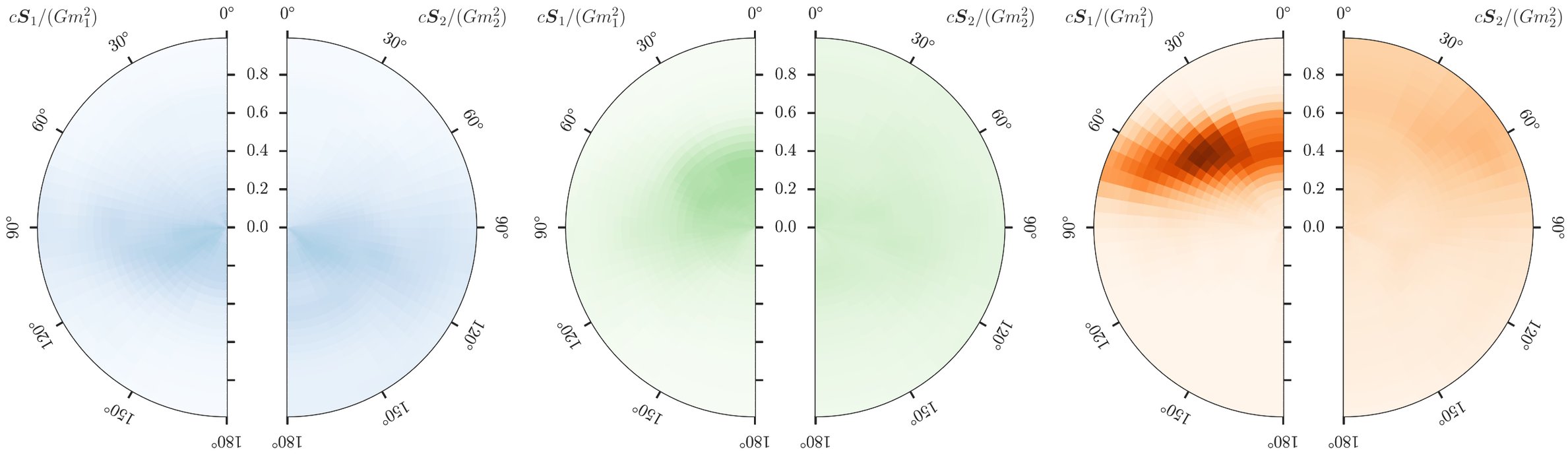

FIG. 5. Posterior probability distributions for the dimensionless component spins $cS_1/(Gm_1^2)$ and $cS_2/(Gm_2^2)$ relative to the normal to the orbital plane L, marginalized over the azimuthal angles. The bins are constructed linearly in spin magnitude and the cosine of the tilt angles, and therefore have equal prior probability. The left plot shows the distribution for GW150914, the middle plot is for LVT151012, and the right plot is for GW151226.

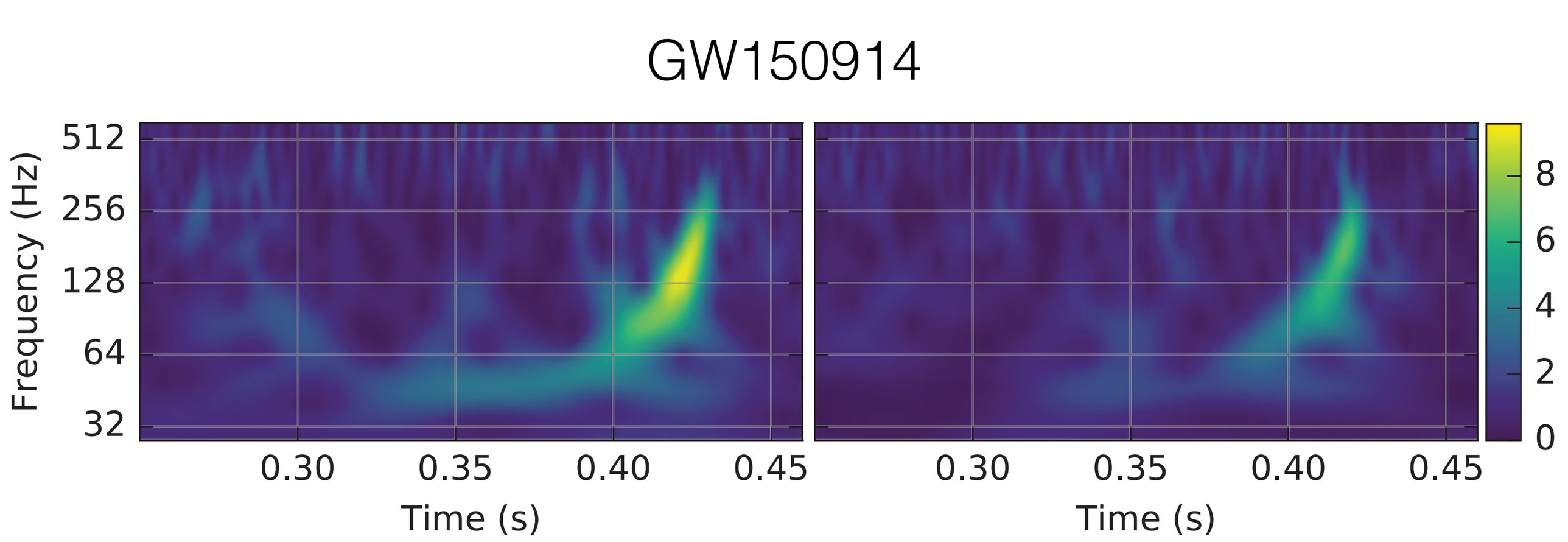
GW150914
Frequency (Hz)
512
256
128
64
32
0.30
0.35
0.40
0.45
Time (s)
0.30
0.35
0.40
0.45
Time (s)
8
6
4
2
0
512
256
128
64
32
−1.0
−0.8
−0.6
−0.4
−0.2
0.0
−1.0
−0.8
−0.6
−0.4
−0.2
0.0
16
14
12
10
8
6
4
2
0
GW151226

2.5 detections so far.

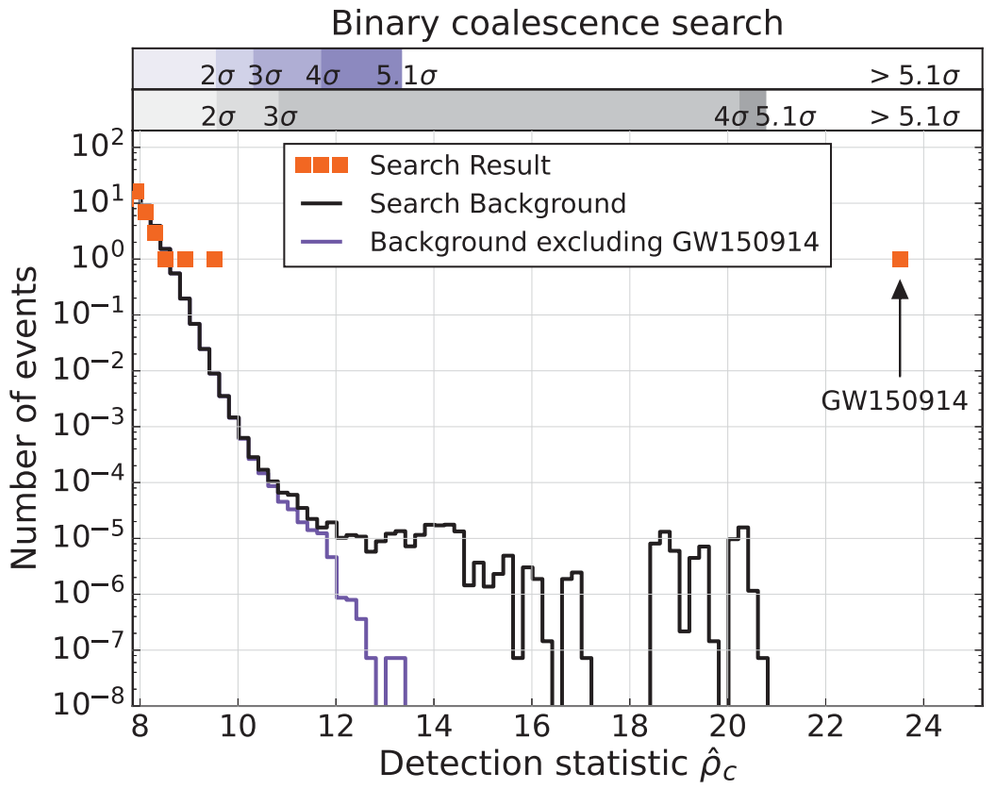

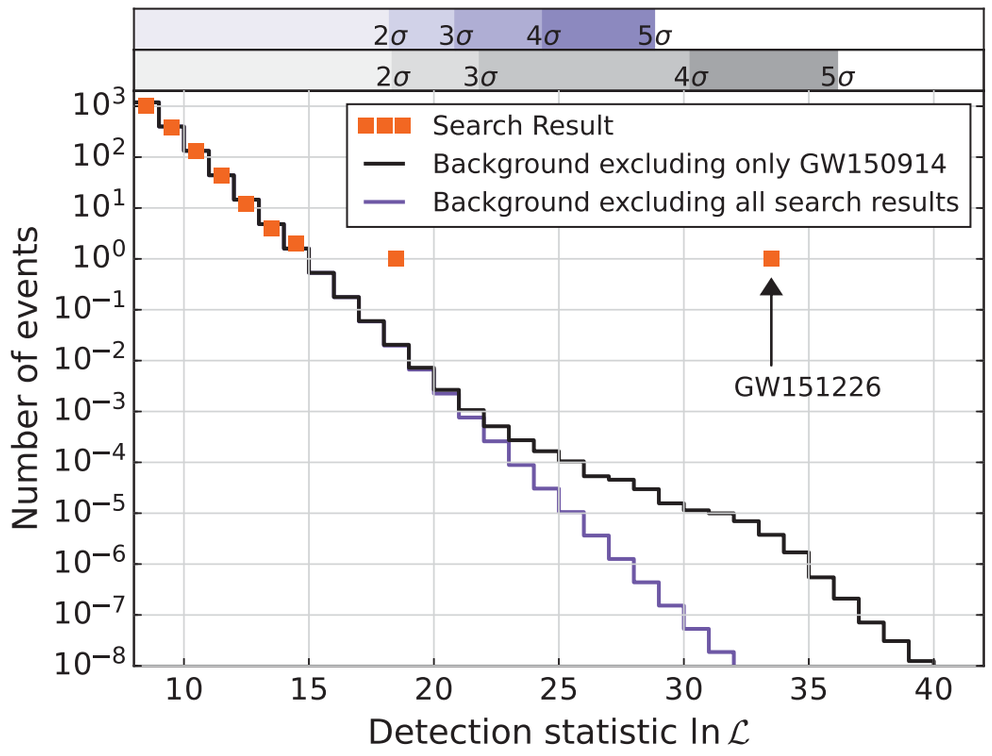

Event Rate Estimates

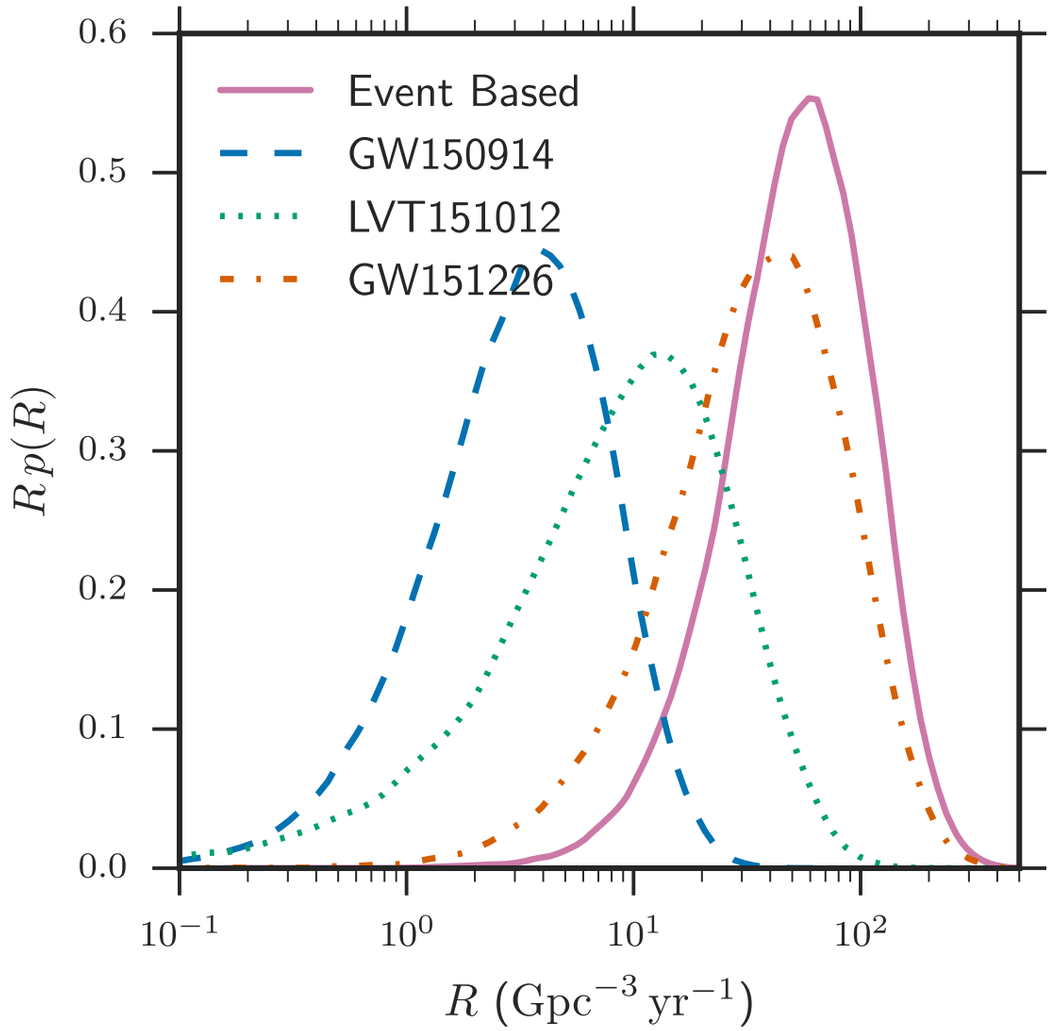

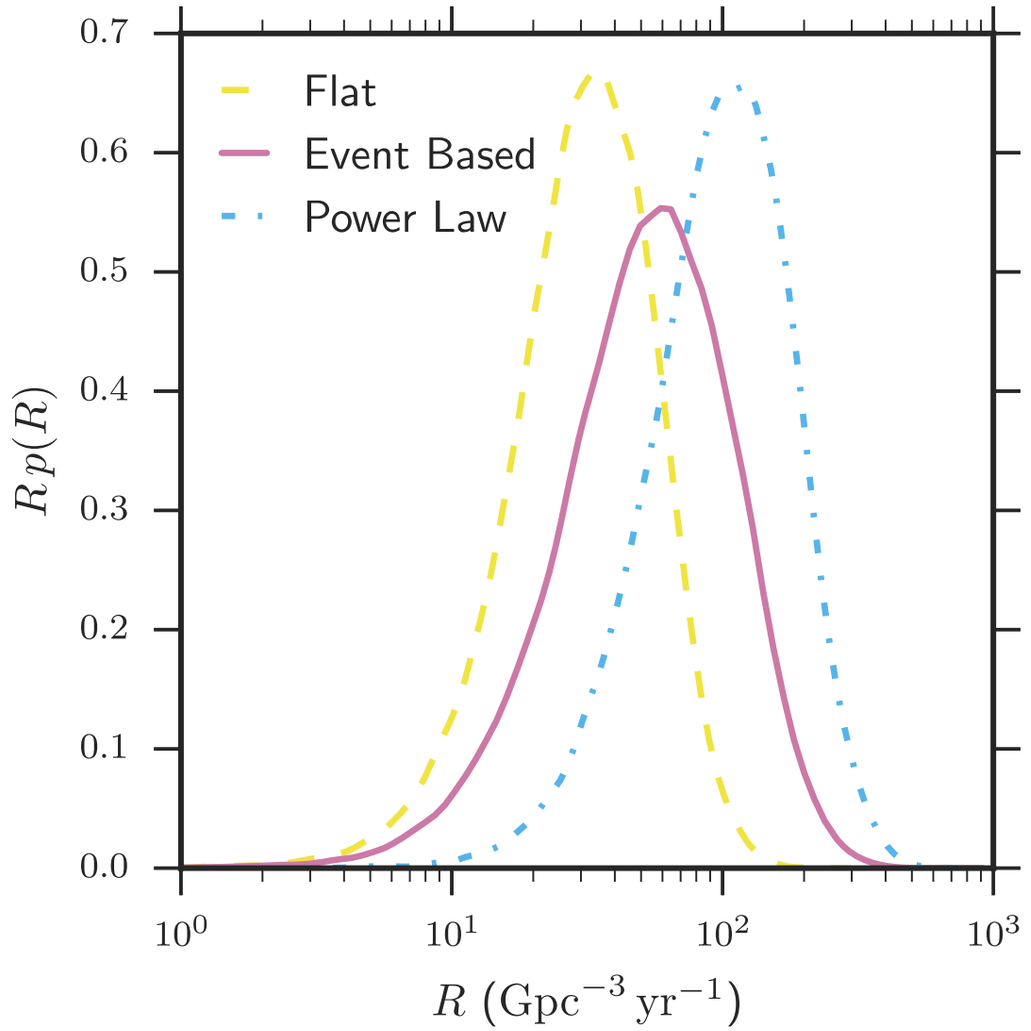

9 - 240 Gpc^{-3}yr^{-1}

Formation Scenarios

The challenge is to create systems with close enough separation to merge within a Hubble time:

- Initial separation:
  - 150914: 50 $R_\odot$
  - 151226: 21 $R_\odot$
  - 151012: 32 $R_\odot$

Field Evolution

The origin and evolution of LIGO's first gravitational-wave source

Krzysztof Belczynski,[1*] Daniel E. Holz,[2] Tomasz Bulik,[1] Richard O'Shaughnessy[3]
[1]Astronomical Observatory, Warsaw University, Ujazdowskie 4, 00-478 Warsaw, Poland
[2]Enrico Fermi Institute, Department of Physics, and Kavli Institute for Cosmological Physics,

15 Feb 2016

Field Evolution

15 Feb 2016

The origin and evolution of LIGO's first gravitational-wave source

Krzysztof Belczynski,[1*] Daniel E. Holz,[2] Tomasz Bulik,[1] Richard O'Shaughnessy[3]
[1]Astronomical Observatory, Warsaw University, Ujazdowskie 4, 00-478 Warsaw, Poland
[2]Enrico Fermi Institute, Department of Physics, and Kavli Institute for Cosmological Physics,

A new route towards merging massive black holes

Pablo Marchant[1⋆], Norbert Langer[1], Philipp Podsiadlowski[2,1], Thomas M. Tauris[1,3], and Takashi J. Moriya[1]

[1] Argelander-Institut für Astronomie, Universität Bonn, Auf dem Hügel 71, 53121 Bonn, Germany
[2] Department of Astrophysics, University of Oxford, Oxford OX1 3RH, UK
[3] Max-Planck-Institut für Radioastronomie, Auf dem Hügel 69, 53121 Bonn, Germany


TIME [Myr]
a [R⊙] e
0.0000
MS
96.2 M⊙
ZAMS
MS
60.2 M⊙
2463
0.15

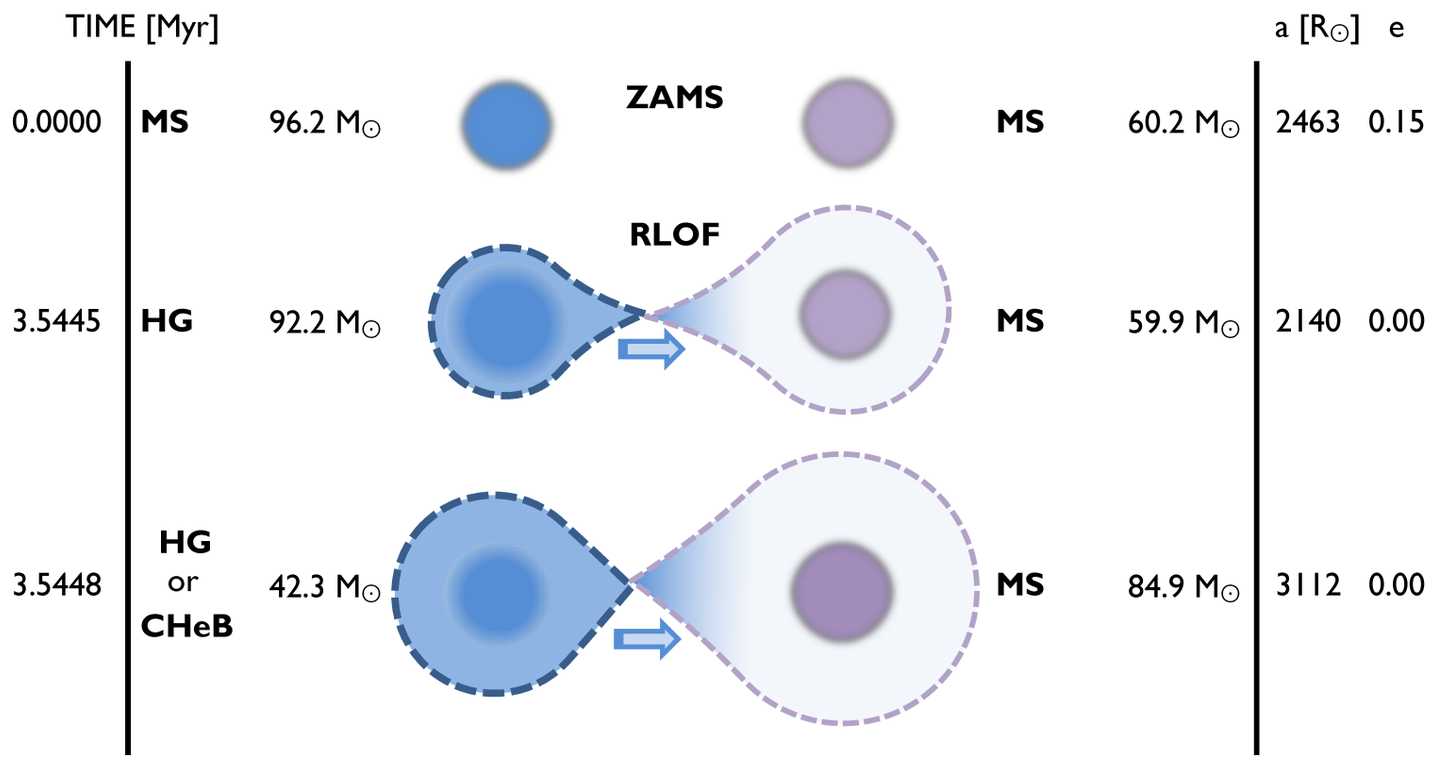
TIME [Myr]
a [R⊙] e
0.0000
MS
96.2 M⊙
ZAMS
MS
60.2 M⊙
2463 0.15
3.5445
HG
92.2 M⊙
RLOF
MS
59.9 M⊙
2140 0.00
3.5448
HG
or
CHeB
42.3 M⊙
MS
84.9 M⊙
3112 0.00

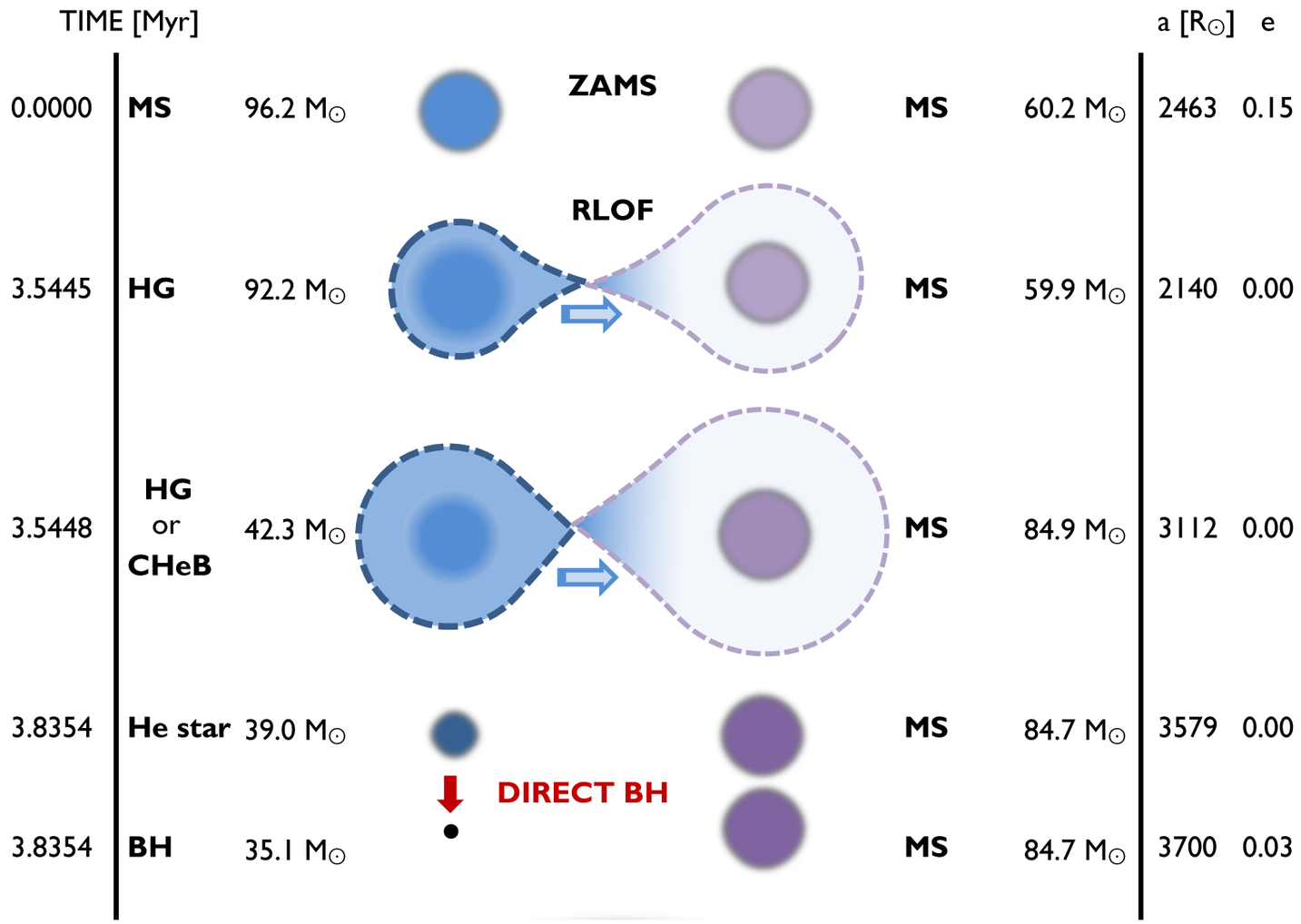
TIME [Myr]
a [R⊙] e
0.0000 MS 96.2 M⊙ ZAMS MS 60.2 M⊙ 2463 0.15
3.5445 HG 92.2 M⊙ RLOF MS 59.9 M⊙ 2140 0.00
3.5448 HG or CHeB 42.3 M⊙ MS 84.9 M⊙ 3112 0.00
3.8354 He star 39.0 M⊙ MS 84.7 M⊙ 3579 0.00
DIRECT BH
3.8354 BH 35.1 M⊙ MS 84.7 M⊙ 3700 0.03

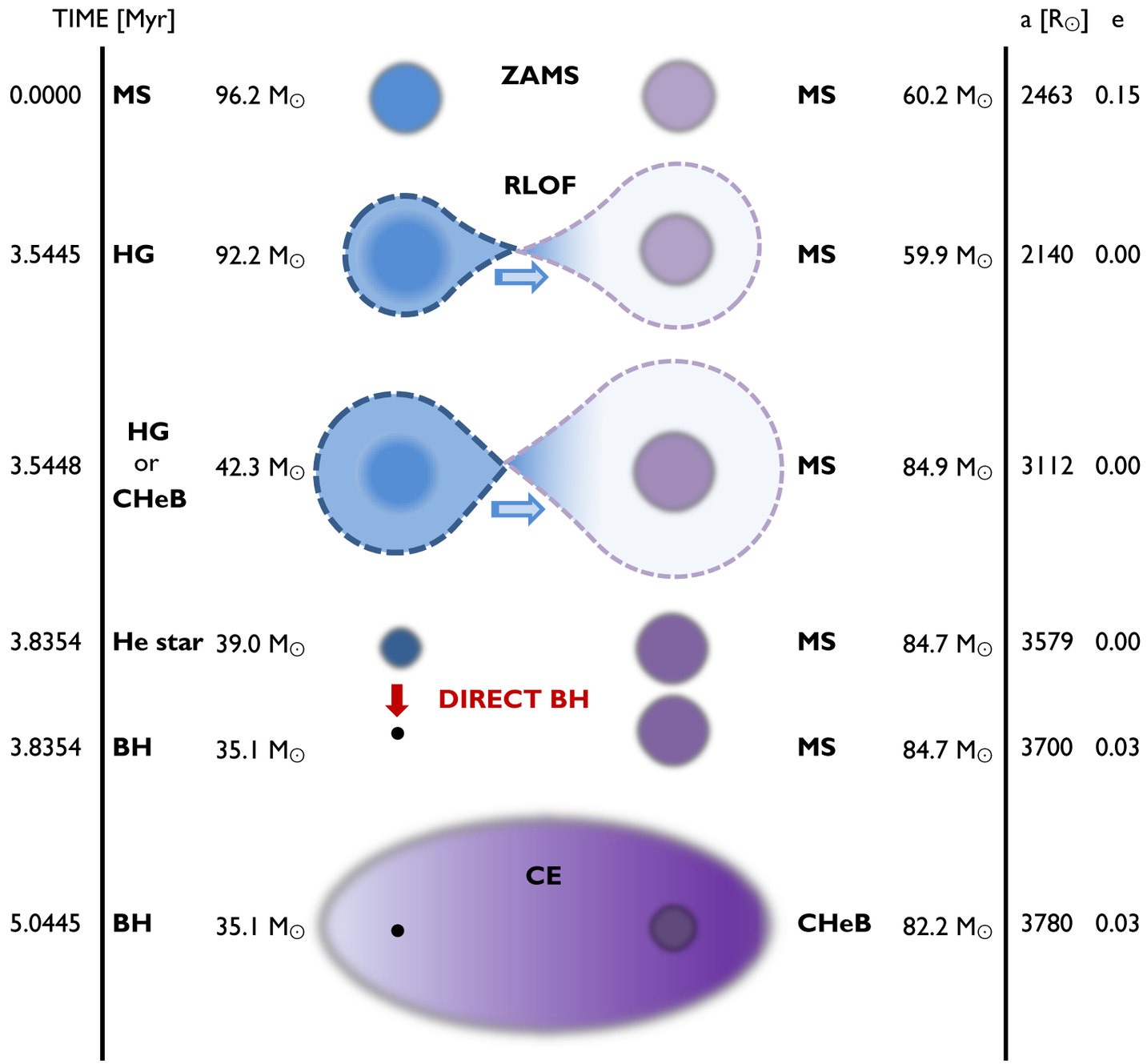
TIME [Myr]
a [R⊙] e
0.0000 MS 96.2 M⊙ ZAMS MS 60.2 M⊙ 2463 0.15
3.5445 HG 92.2 M⊙ RLOF MS 59.9 M⊙ 2140 0.00
3.5448 HG or CHeB 42.3 M⊙ MS 84.9 M⊙ 3112 0.00
3.8354 He star 39.0 M⊙ MS 84.7 M⊙ 3579 0.00
DIRECT BH
3.8354 BH 35.1 M⊙ MS 84.7 M⊙ 3700 0.03
5.0445 BH 35.1 M⊙ CE CHeB 82.2 M⊙ 3780 0.03

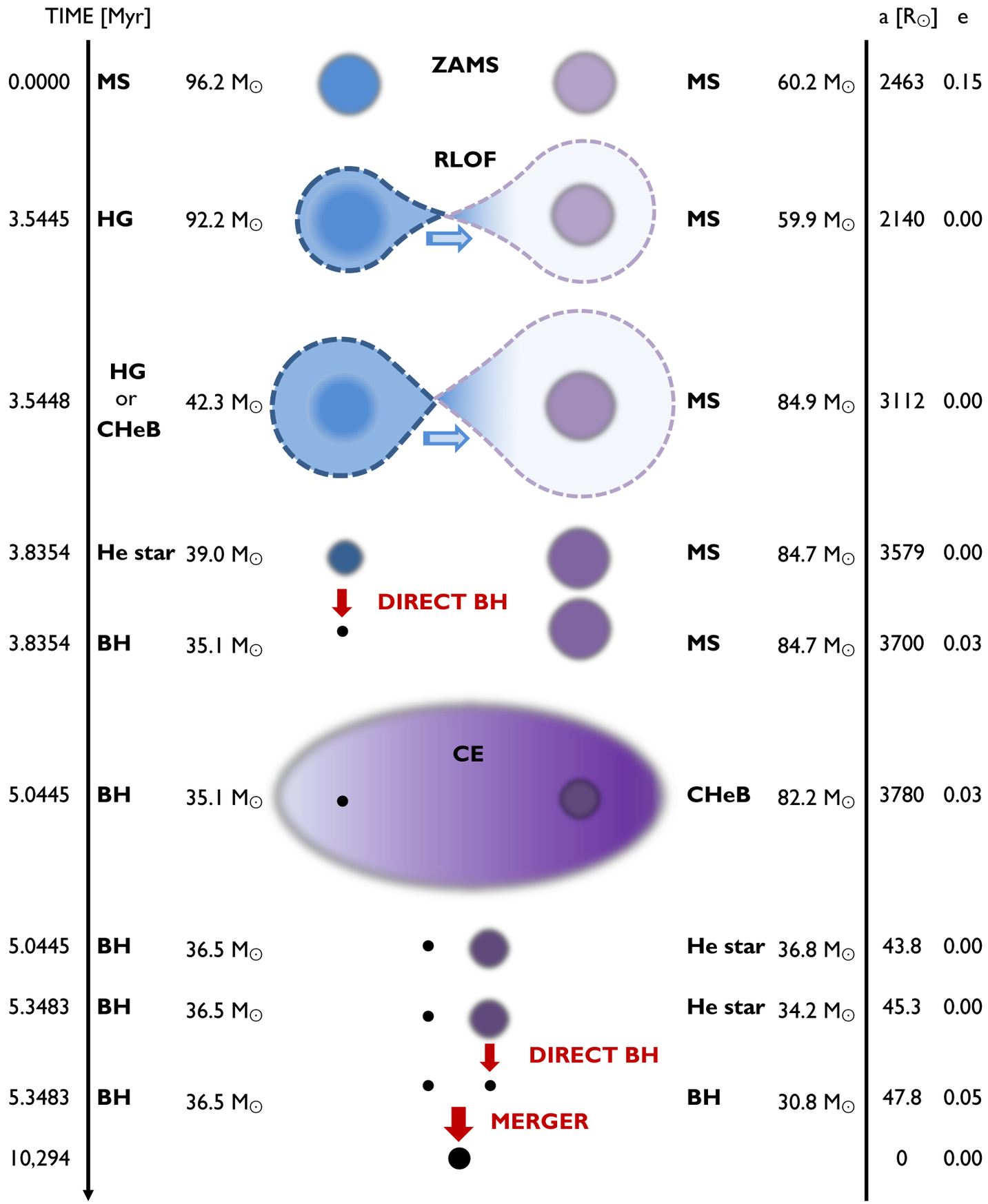
TIME [Myr]
a [R⊙] e
0.0000 MS 96.2 M⊙ ZAMS MS 60.2 M⊙ 2463 0.15
3.5445 HG 92.2 M⊙ RLOF MS 59.9 M⊙ 2140 0.00
3.5448 HG or CHeB 42.3 M⊙ MS 84.9 M⊙ 3112 0.00
3.8354 He star 39.0 M⊙ MS 84.7 M⊙ 3579 0.00
DIRECT BH
3.8354 BH 35.1 M⊙ MS 84.7 M⊙ 3700 0.03
CE
5.0445 BH 35.1 M⊙ CHeB 82.2 M⊙ 3780 0.03
5.0445 BH 36.5 M⊙ He star 36.8 M⊙ 43.8 0.00
5.3483 BH 36.5 M⊙ He star 34.2 M⊙ 45.3 0.00
DIRECT BH
5.3483 BH 36.5 M⊙ BH 30.8 M⊙ 47.8 0.05
MERGER
10,294 0 0.00

MODEL

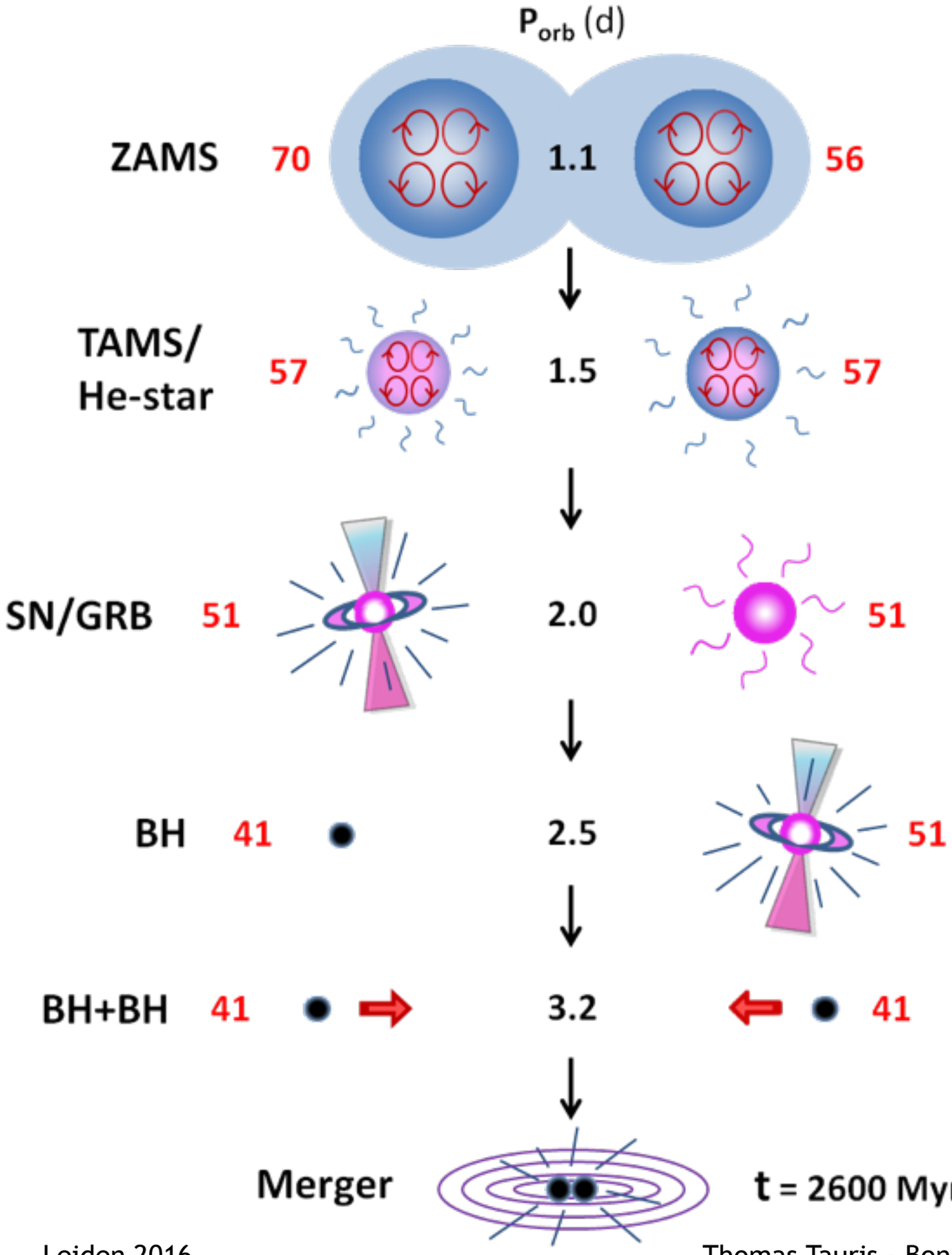
P_{orb} (d)
ZAMS
70
1.1
56
TAMS/
He-star
57
1.5
57
SN/GRB
51
2.0
51
BH
41
2.5
51
BH+BH
41
3.2
41
Merger
t = 2600 Myr

MODEL

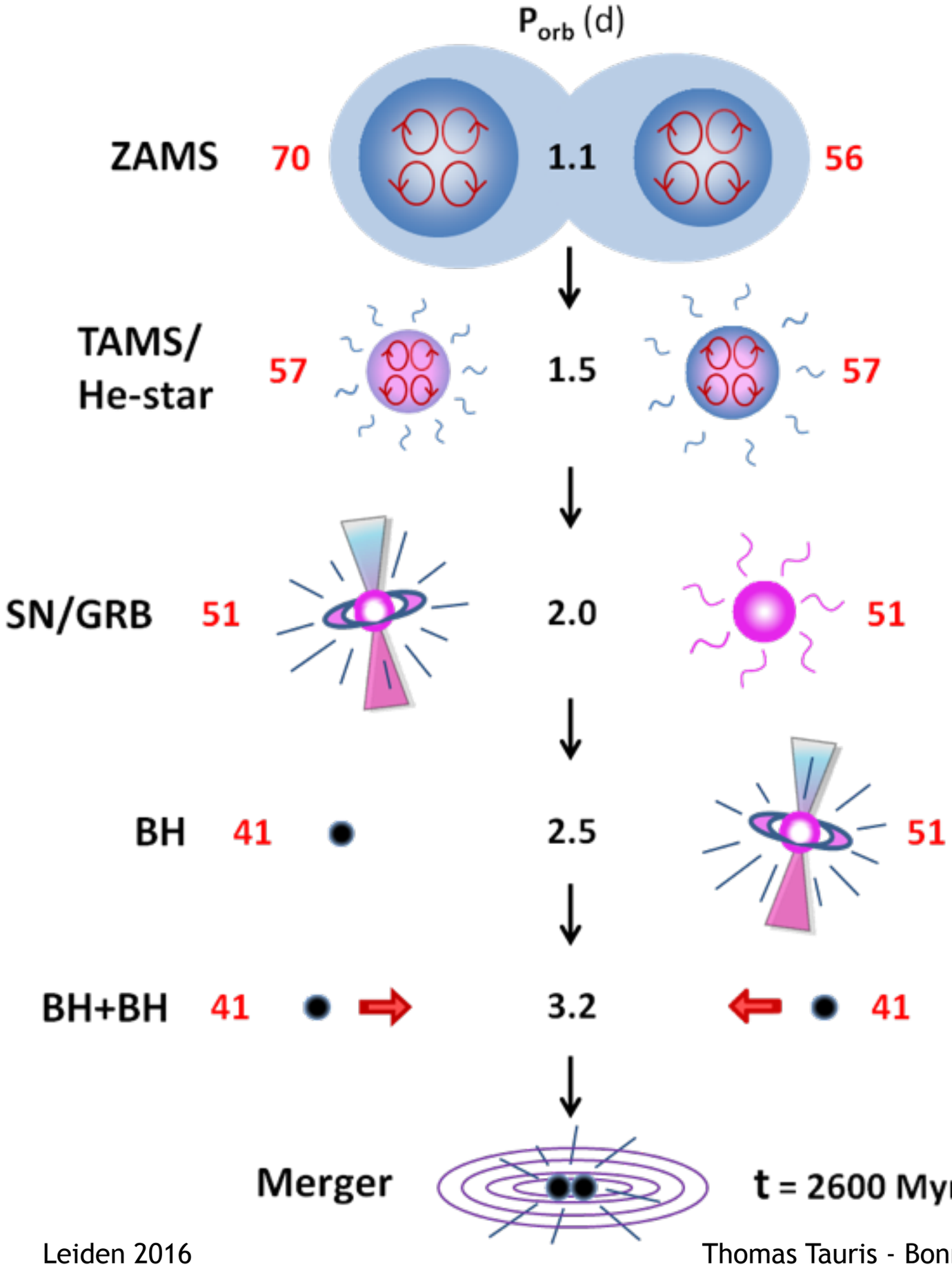
P_{orb} (d)
ZAMS
70
1.1
56
TAMS/
He-star
57
1.5
57
SN/GRB
51
2.0
51
BH
41
2.5
51
BH+BH
41
3.2
41
Merger
t = 2600 Myr

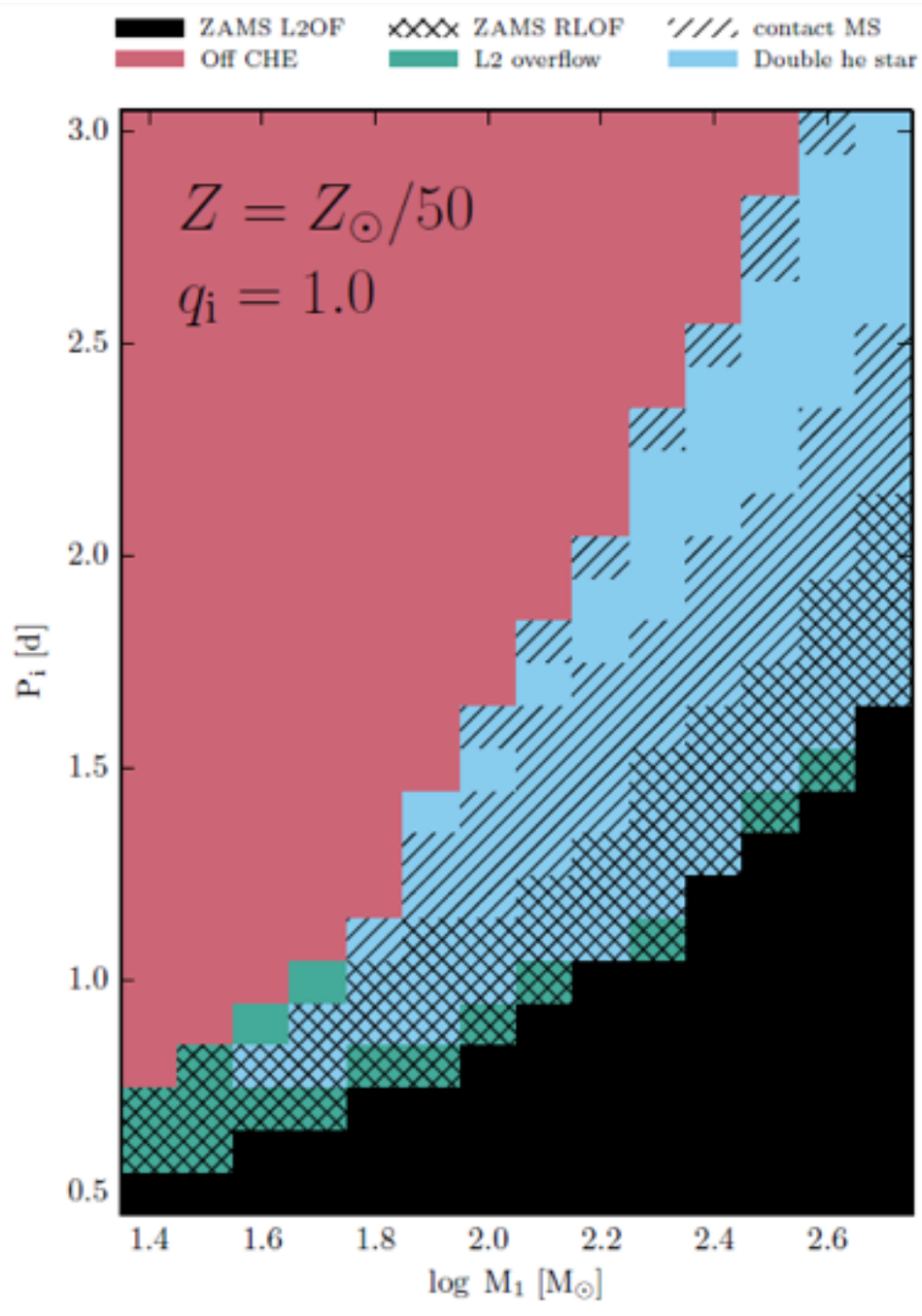
ZAMS L2OF
Off CHE
ZAMS RLOF
L2 overflow
contact MS
Double he star
$Z = Z_\odot/50$
$q_i = 1.0$
P_i [d]
3.0
2.5
2.0
1.5
1.0
0.5
1.4
1.6
1.8
2.0
2.2
2.4
2.6
log M_1 [$M_\odot$]

Draft version March 4, 2016
Preprint typeset using LaTeX style emulateapj v. 5/2/11

BINARY BLACK HOLES IN DENSE STAR CLUSTERS: EXPLORING THE THEORETICAL UNCERTAINTIES

Sourav Chatterjee, Carl L. Rodriguez, & Frederic A. Rasio
Center for Interdisciplinary Exploration & Research in Astrophysics (CIERA)
Physics & Astronomy, Northwestern University, Evanston, IL 60202, USA
sourav.chatterjee@northwestern.edu

Draft version March 4, 2016

Portegies Zwart & McMillan 2000
Miller & Hamilton 2002
MB 2002
O'Leary + 2006
O'Leary, O'Shaughnessy, & Rasio 2007
Sadowski + 2008
Moody & Sigurdsson 2009
Downing, MB, Giersz, & Spurzem 2010
Downing, MB, Giersz, & Spurzem 2011
Morscher, Umbreit, Farr, Rasio 2013
Bae, Kim, & Lee 2014

Draft version March 4, 2016
Preprint typeset using LaTeX style emulateapj v. 5/2/11

BINARY BLACK HOLES IN DENSE STAR CLUSTERS: EXPLORING THE THEORETICAL UNCERTAINTIES

Sourav Chatterjee, Carl L. Rodriguez, & Frederic A. Rasio
Center for Interdisciplinary Exploration & Research in Astrophysics (CIERA)
Physics & Astronomy, Northwestern University, Evanston, IL 60202, USA
sourav.chatterjee@northwestern.edu

Draft version March 4, 2016

Other Talks in This Session

Portegies Zwart & McM
Miller & Hamilton 2
MB 2002
O'Leary +
O'Lea essy, & Rasio 2007
Sa d
gurdsson 2009
g, MB, Giersz, & Spurzem 2010
wning, MB, Giersz, & Spurzem 2011
Morscher, Umbreit, Farr, Rasio 2013
Bae, Kim, & Lee 2014

Summary

- Gravitational wave observations give
  - Masses
  - Inclination
  - Distance
  - Spin

- Difficulties
  - Sky location
  - Spins are difficult
  - Formation ? Kicks ?

Prospects for eLISA

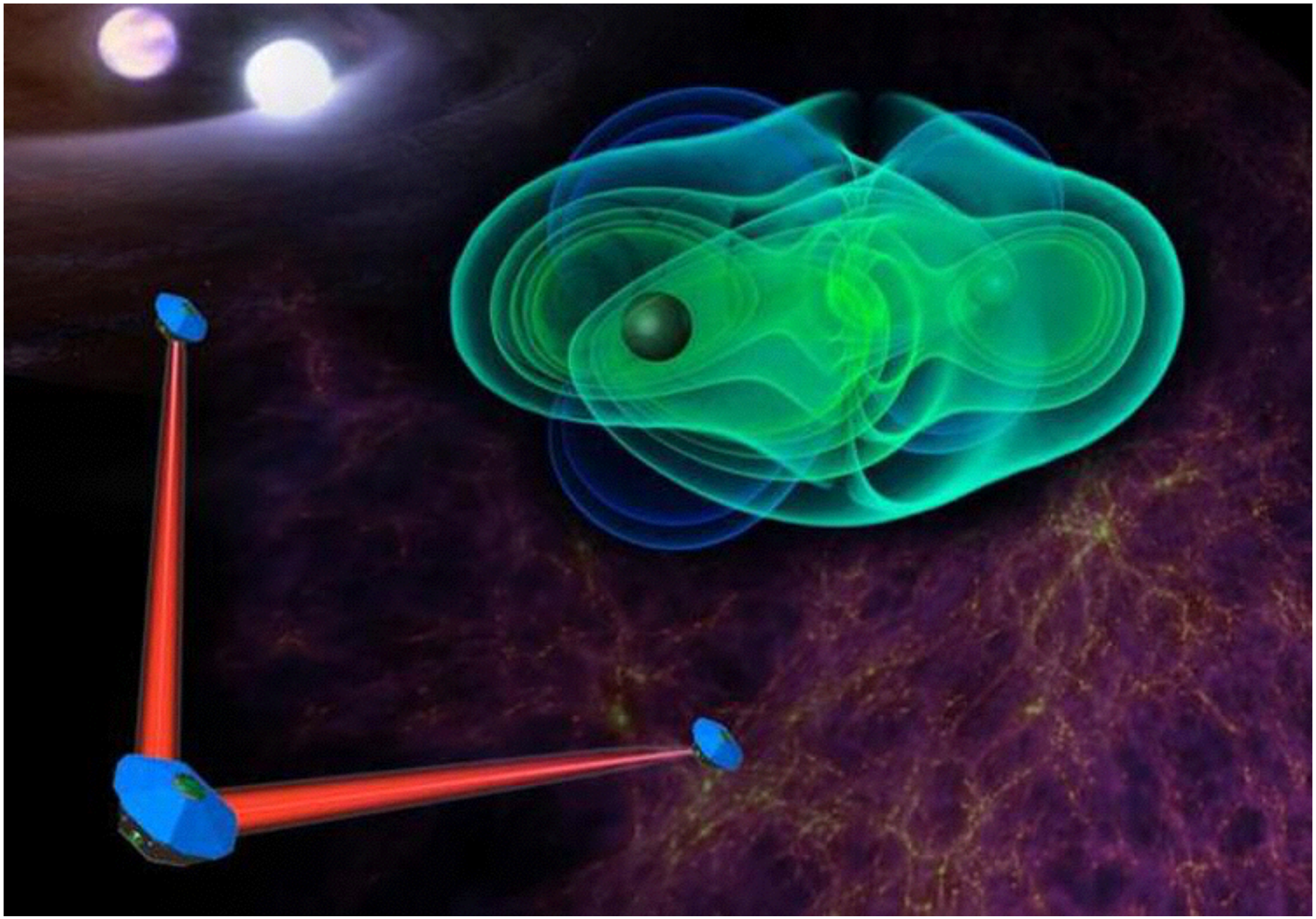

If a binary black hole merges, this implies that there are many more binary black holes at lower frequencies.

These will be eLISA sources

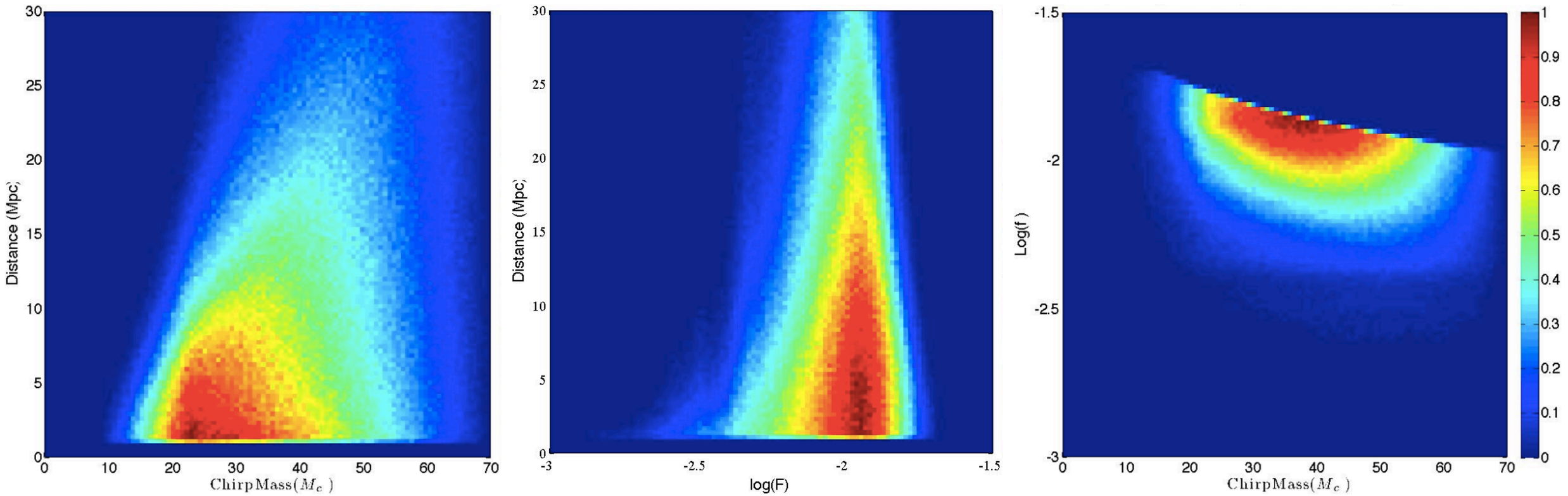

MB, Hinojosa, Mata, Belczynski 2015

- Frequency evolution of a binary: $\dot{f} = k_0 f^{11/3}$

$$k_0 = \frac{96}{5} (2\pi)^{8/3} \frac{G^{5/3}}{c^5} \frac{m_1 m_2}{M^{1/3}}$$

- Number density of binaries in frequency range *df:*

$$dn = \frac{\eta}{k_0} f^{-11/3} df$$

- Number density of binaries above $f_{\rm min}$:

$$n = \frac{\eta}{k_0} \frac{3}{8} f_{\rm min}^{-8/3}$$

Volume to 30 Mpc and minimum frequency of 1 mHz.

Merger rate in events/Gpc^3/yr.

All systems with same chirp mass.

The number of systems in this volume is numerically equal to the merger rate.

Expect more than 2-400 systems within 30 Mpc in the eLISA band.

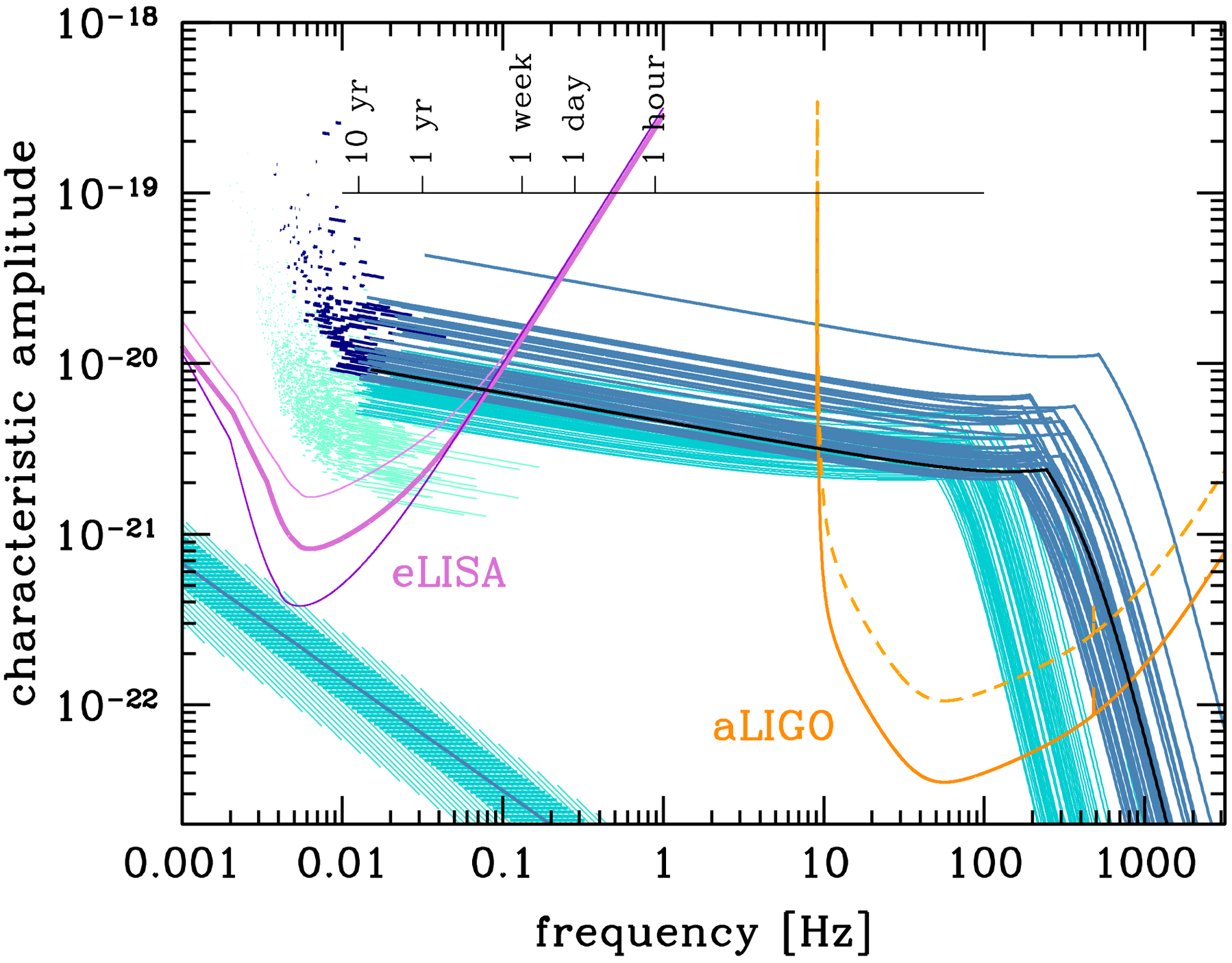
characteristic amplitude
frequency [Hz]
10 yr
1 yr
1 week
1 day
1 hour
eLISA
aLIGO
0.001
0.01
0.1
1
10
100
1000
10^{-18}
10^{-19}
10^{-20}
10^{-21}
10^{-22}

Sesana 2016

eLISA error box superimposed on a chart of the Virgo cluster, centered on NGC 4365 for a typical BBH signal.

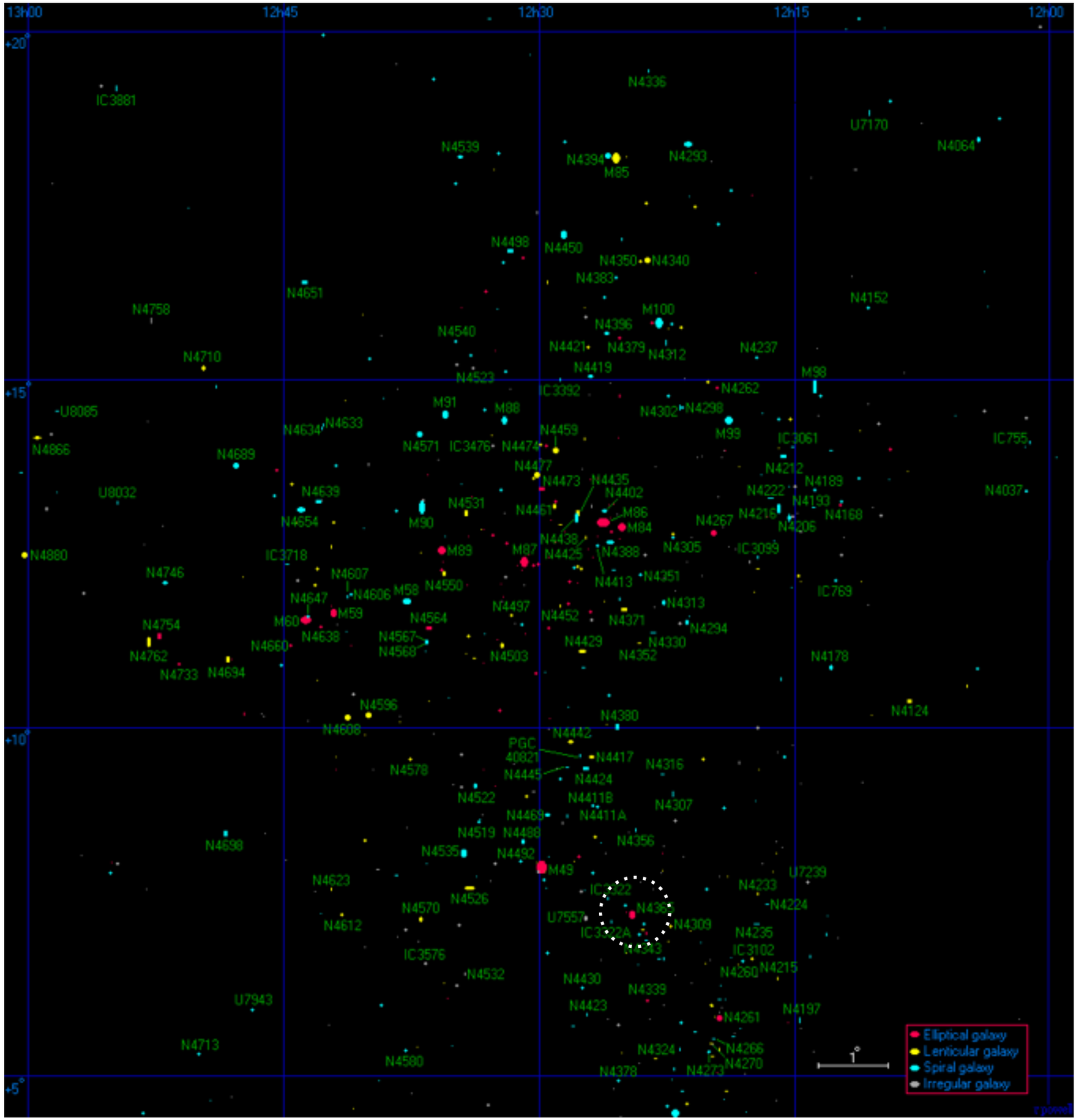

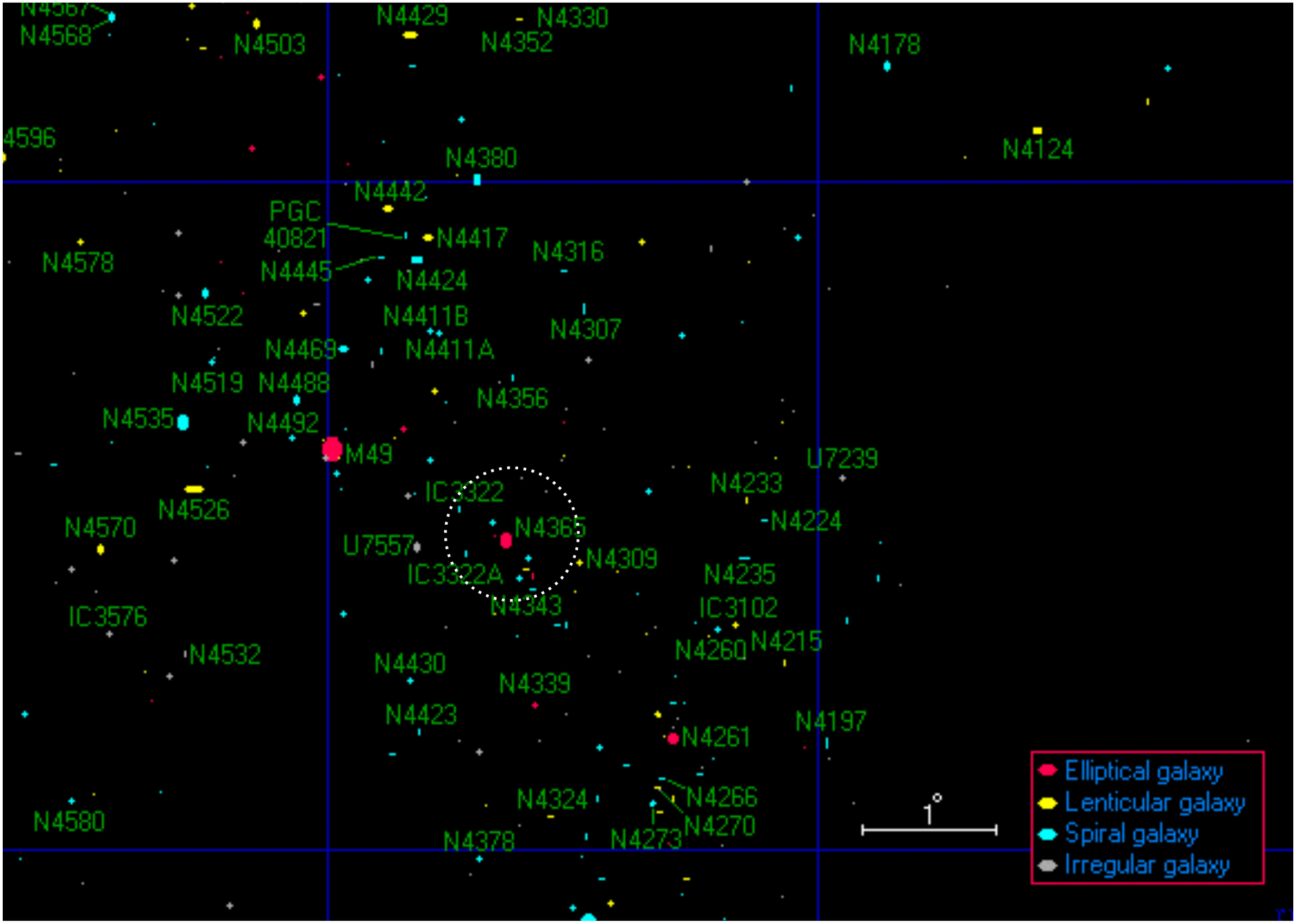
N4568
N4503
N4429
N4330
N4352
N4178
4596
N4124
N4380
N4442
PGC
40821
N4417
N4316
N4578
N4445
N4424
N4522
N4411B
N4307
N4469
N4411A
N4519
N4488
N4356
N4535
N4492
M49
U7239
IC3322
N4233
N4526
N4570
N4365
-N4224
U7557
N4309
IC3322A
N4235
N4343
IC3576
IC3102
N4260
N4215
N4532
N4430
N4339
N4423
N4197
N4261
N4324
N4266
N4580
N4270
N4378
N4273
1°
Elliptical galaxy
Lenticular galaxy
Spiral galaxy
Irregular galaxy